JIDOpen

C1r Upregulates Production of Matrix Metalloproteinase-13 and Promotes Invasion of Cutaneous Squamous Cell Carcinoma

Kristina Viiklepp[1,2], Liisa Nissinen[1,2], Marjaana Ojalill[3], Pilvi Riihilä[1,2], Markku Kallajoki[4], Seppo Meri[5,6], Jyrki Heino[3] and Veli-Matti Kähäri[1,2]

Cutaneous squamous cell carcinoma (cSCC) is the most common metastatic skin cancer, with increasing incidence worldwide. Previous studies have shown the role of the complement system in cSCC progression. In this study, we have investigated the mechanistic role of serine proteinase C1r, a component of the classical pathway of the complement system, in cSCC. Knockout of C1r in cSCC cells using CRISPR/Cas9 resulted in a significant decrease in their proliferation, migration, and invasion through collagen type I compared with that of wild-type cSCC cells. Knockout of C1r suppressed the growth and vascularization of cSCC xenograft tumors and promoted apoptosis of tumor cells in vivo. mRNA-sequencing analysis after C1r knockdown revealed significantly regulated Gene Ontology terms cell-matrix adhesion, extracellular matrix component, basement membrane, and metalloendopeptidase activity and Kyoto Encyclopedia of Genes and Genomes pathway extracellular matrix–receptor interaction. Among the significantly regulated genes were invasion-associated matrix metalloproteinases (MMPs) *MMP1*, *MMP13*, *MMP10*, and *MMP12*. Knockout of C1r resulted in decreased production of MMP-1, MMP-13, MMP-10, and MMP-12 by cSCC cells in culture. Knockout of C1r inhibited the expression of MMP-13 by tumor cells, suppressed invasion, and reduced the amount of degraded collagen in vivo in xenografts. These results provide evidence for the role of C1r in promoting the invasion of cSCC cells by increasing MMP production.

Journal of Investigative Dermatology (2021) ■, ■–■; doi:10.1016/j.jid.2021.10.008

INTRODUCTION

Epidermal keratinocyte–derived cutaneous squamous cell carcinoma (cSCC) is the most common skin cancer with metastatic potential. It is the second most common skin cancer after basal cell carcinoma, and its incidence is increasing all over the world (Nehal and Bichakjian, 2018). The estimated metastasis rate of primary cSCC is 3–5%, and the prognosis of metastatic cSCC is poor because >70% will die of the disease within 3 years (Knuutila et al., 2020; Nagarajan et al., 2019). Accordingly, cSCC has been estimated to cause 20% of skin cancer–related mortality (Karia et al., 2013; Nehal and Bichakjian, 2018; Que et al., 2018). cSCC develops from premalignant lesion, actinic keratosis, to cSCC in situ (Bowen's disease) and finally to invasive and metastatic cSCC. The main predisposing factors for the development and progression of cSCC are long-term exposure to solar UVR, immunosuppression, chronic inflammation, and chronic dermal ulcers (Ratushny et al., 2012).

The complement system is an important part of the innate immune system (Abu-Humaidan et al., 2014; Ricklin et al., 2010; Rutkowski et al., 2010). It connects innate and acquired immunity and serves as the first line of host defense. The complement system is activated through three distinct pathways, that is, classical, lectin, and alternative pathways, in response to the influx of microbes or to tissue injury. All the three pathways converge in cleavage of the central component C3 to C3a and C3b fragments. C3b binds covalently to target cells and launches the activation of the terminal pathway and formation of the lytic membrane attack complex (Bohlson et al., 2019; Riihilä et al., 2019).

Activation of the classical pathway of complement is typically initiated by binding of $C1qr_2s_2$ complex to a complement-fixing antibody cluster of IgM or IgG bound to the antigen on target cells. The C1 complex contains C1q and two subcomponents C1r and C1s. The large C1q molecule is composed of six collagenous triple helices, each with C1qA, C1qB, and C1qC subunits. In addition to the collagenous tails, C1q contains six globular head regions. Activation of the $C1qr_2s_2$ complex is initiated by binding of the C1q globular heads to structures on microbial, necrotic, and apoptotic cells or to Igs and pentraxins, such as CRP, which launch a stepwise autocatalytic activation of the serine

[1]Department of Dermatology, University of Turku and Turku University Hospital, Turku, Finland; [2]FICAN West Cancer Centre Laboratory, University of Turku and Turku University Hospital, Turku, Finland; [3]Department of Life Technologies, University of Turku, Turku, Finland; [4]Department of Pathology, University of Turku and Turku University Hospital, Turku, Finland; [5]Department of Bacteriology and Immunology, University of Helsinki, Helsinki, Finland; and [6]Translational Immunology Research Program, University of Helsinki, Helsinki, Finland

Correspondence: Veli-Matti Kähäri, Department of Dermatology, University of Turku and Turku University Hospital, Hämeentie 11 TE6, FI-20520 Turku, Finland. E-mail: veli-matti.kahari@utu.fi

Abbreviations: CHP, collagen hybridizing peptide; cSCC, cutaneous squamous cell carcinoma; ECM, extracellular matrix; ERK, extracellular signal–regulated kinase; KO, knockout; MMP, matrix metalloproteinase; siRNA, short interfering RNA; VG, van Gieson; WT, wild type

Received 17 December 2020; revised 1 October 2021; accepted 4 October 2021; accepted manuscript published online XXX; corrected proof published online XXX

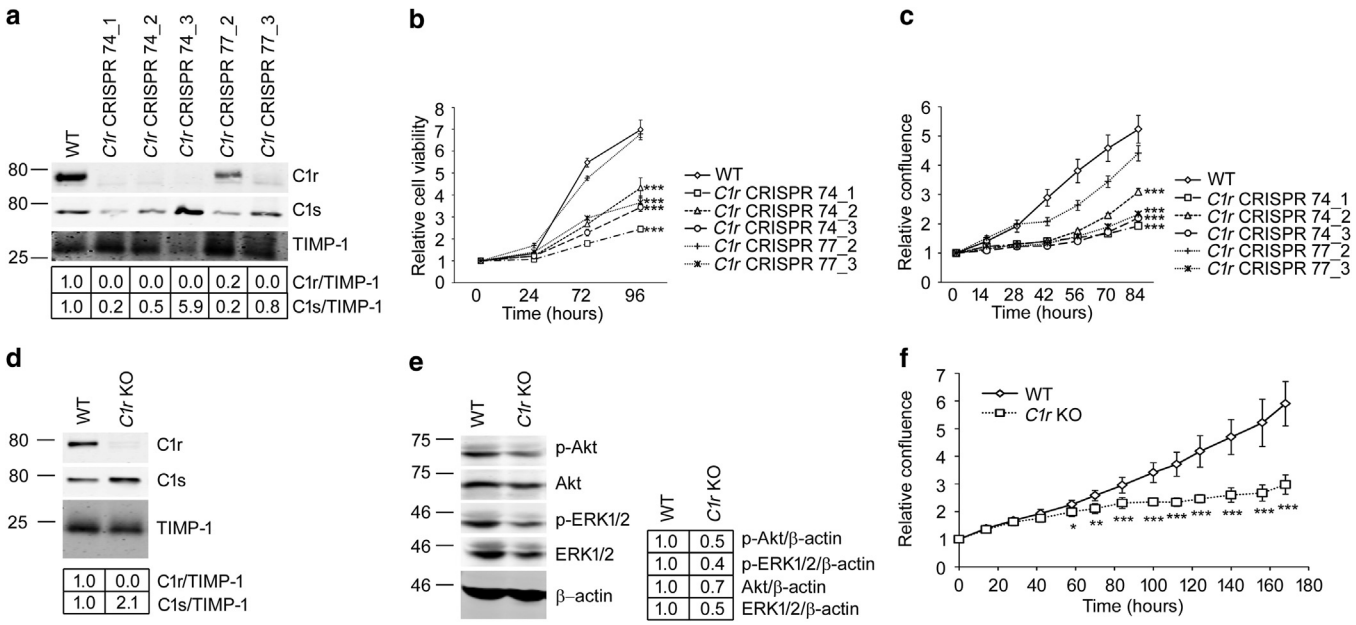

Figure 1. KO of C1r suppresses the proliferation of cSCC cells. (**a**) Conditioned media of CRISPR/Cas9-treated UT-SCC-7 single-cell clones and WT UT-SCC-7 cells were analyzed by western blotting for the levels of C1r and C1s. TIMP-1 was determined as the loading control. (**b**) The number of viable UT-SCC-7 single-cell clones and WT UT-SCC-7 cells was determined at the time points indicated using WST-1 assay (n = 8). (**c**) The confluency of UT-SCC-7 single-cell clones and WT cells was determined using IncuCyte ZOOM (n = 8) (**d**) The levels of C1r and C1s in conditioned media, and (**e**) the levels of p-Akt, p-ERK1/2, total Akt, and total ERK1/2 in cell lysates of C1r-KO cell pools and UT-SCC-7 cSCC-WT cells were determined by western blotting. TIMP-1 or β-actin was used as the loading control. Quantitations of the western blots corrected for loading controls are shown below the panels. (**f**) The confluency of the C1r-KO and -WT UT-SCC-7 cells was determined using IncuCyte ZOOM (n = 8). $*P < 0.05$, $**P < 0.01$, $***P < 0.001$ by Student's *t*-test. Akt, protein kinase B; cSCC, cutaneous squamous cell carcinoma; ERK, extracellular signal–regulated kinase; KO, knockout; p-Akt, phosphorylated protein kinase B; p-ERK, phosphorylated extracellular signal–regulated kinase; WT, wild type.

proteinase C1r, which in turn activates C1s (Navratil et al., 2001; Venkatraman Girija et al., 2013). C1s subsequently cleaves serum proteins C4 and C2 to C4a and C4b and C2a and C2b fragments, respectively. The complex C4b2b, also known as the classical pathway C3 convertase, then activates C3 and initiates the lytic pathway (Bohlson et al., 2019; Ricklin et al., 2010). It has been recently shown that tumor cell–derived complement components exert cancer-promoting properties and play a role in cancer progression, independently of complement activation (Afshar-Kharghan, 2017; Reis et al., 2018; Riihilä et al., 2019; Roumenina et al., 2019).

We have previously shown significant upregulation of complement components in tumor cells in cSCC in vivo and in cSCC cell lines (Riihilä et al., 2020, 2017, 2015, 2014). Recently, we showed that components of the classical pathway, C1r and C1s, are significantly upregulated in tumor cells in cSCC in vivo (Riihilä et al., 2020). In this study, we have specifically investigated the mechanistic role of serine proteinase C1r in the progression of cSCC. For this, we generated C1r-negative cSCC cells using CRISPR/Cas9. Knockout (KO) of C1r inhibited cSCC cell proliferation, migration, and invasion through collagen type I. Furthermore, KO of C1r suppressed the growth and vascularization of cSCC xenograft tumors and promoted the apoptosis of tumor cells in vivo. KO of C1r resulted in significant downregulation in the expression of invasion-associated matrix metalloproteinases (MMPs) MMP-1, MMP-13, MMP-10, and MMP-12 by cSCC cells. KO of C1r also inhibited the expression of MMP-13 by tumor cells, suppressed invasion, and reduced the amount of degraded collagen in vivo in xenografts. These results provide evidence for the role of C1r in promoting the invasion of cSCC cells by increasing MMP production.

RESULTS

KO of C1r decreases the proliferation of cSCC cells

C1r-negative cSCC cells were generated of metastatic human cSCC cell line (UT-SCC-7) using CRISPR/Cas9. Analysis of conditioned media with western blotting confirmed loss of C1r in four cSCC single-cell clones, whereas the production of C1s was not abolished (Figure 1a). The KO of C1r was also confirmed by sequencing the PCR product obtained by amplification of genomic DNA of single-cell clones in the corresponding area (Supplementary Figure S1). C1r-KO resulted in a significant decrease in the viability (Figure 1b) and growth (Figure 1c) of cSCC cell clones. Four C1r KO cSCC single-cell clones (C1r CRISPR 74_1, 74_2, 74_3, and 77_3) were pooled, and the expression of C1r and C1s in pooled cells (C1r-KO) was confirmed using western blotting (Figure 1d). Cell lysates of C1r-KO and –wild-type (WT) cSCC cells showed decreased protein levels of protein kinase B (Akt) and extracellular signal–regulated kinase (ERK) 1/2 in C1r-KO cells, and this resulted in decreased levels of phosphorylated Akt and ERK1/2 (Figure 1e). In addition, a significant decrease in the growth of C1r-KO compared with that in WT cSCC cells was noted (Figure 1f).

KO of C1r suppresses the growth of cSCC in vivo

C1r-KO and cSCC-WT cells (UT-SCC-7) were injected (7×10^6 cells) subcutaneously into the back of SCID mice (n = 6

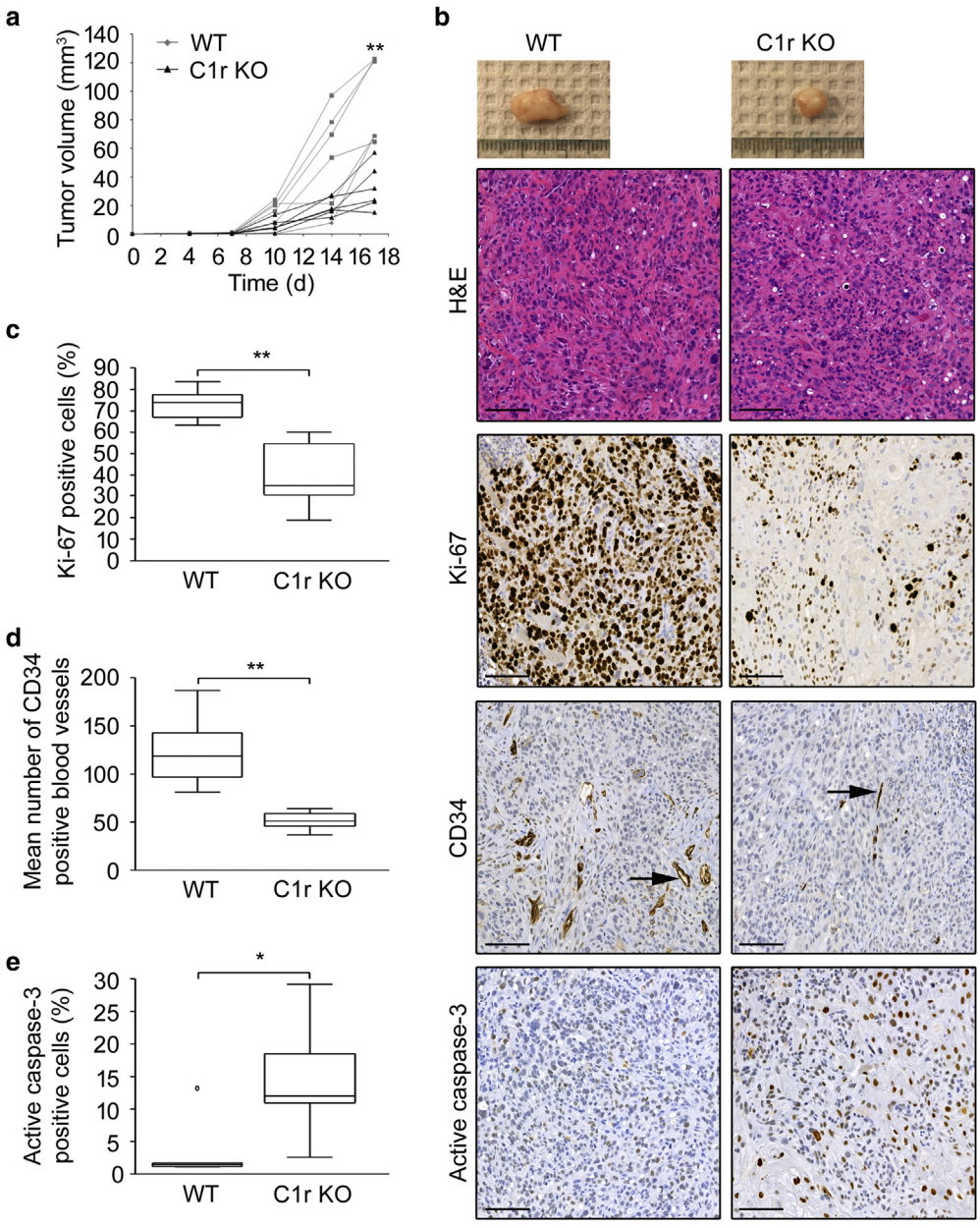

Figure 2. KO of C1r suppresses the growth of cSCC in vivo. C1r-KO or -WT UT-SCC-7 cells (7×10^6 cells) were injected subcutaneously into the back of SCID mice, and (**a**) the size of tumors was measured twice a week (n = 6 in both groups). $^{**}P < 0.01$ by Mann–Whitney U-test. (**b**) Xenografts were harvested after 17 days and stained with H&E, and with immunohistochemistry for the proliferation marker Ki-67, the vascular endothelial marker CD34, and the apoptosis marker active caspase-3, with Mayer's hematoxylin as counterstain. Representative stainings from each group are shown. Arrows indicate CD34-positive blood vessels. Bar = 100 μm. (**c**) The percentage of Ki-67–positive cells, (**d**) the number of CD34-positive blood vessels, and (**e**) the percentage of active caspase-3–positive cells were counted. (n = 6 in both groups) $^{*}P < 0.05$, $^{**}P < 0.01$ by Mann–Whitney U-test. cSCC, cutaneous squamous cell carcinoma; d, day; KO, knockout; WT, wild type.

in both groups). The growth of C1r-KO xenograft tumors was significantly reduced, compared with that of WT tumors (Figure 2a and b). The relative number of proliferating Ki-67–positive cells (Figure 2b and c) and the number of CD34-positive blood vessels were significantly lower in C1r-KO tumors (Figure 2b and d). The percentage of active caspase-3–positive apoptotic cells was significantly higher in C1r-KO tumors than in WT tumors (Figure 2b and e).

Alteration of gene expression profile in C1r-knockdown cSCC cells

C1r expression was knocked down in three cSCC cell lines with short interfering RNA (siRNA) (Supplementary Figure S2), and gene expression profiling was performed by mRNA sequencing. Knockdown of C1r significantly decreased the mRNA levels of *C1R*, *C1RL* (complement *C1r* subcomponent like), and MAC-inhibitory protein (*CD59*), whereas the levels of mRNAs for other complement components, including C1s, was not altered (Supplementary Figure S3). The genes significantly regulated after C1r knockdown were associated with Gene Ontology terms cell-matrix adhesion, extracellular matrix (ECM) component, basement membrane, and metallopeptidase activity and with Kyoto Encyclopedia of Genes and Genomes pathway ECM–receptor interaction (Figure 3a). Expression of genes coding for several MMPs and integrins was significantly regulated in Gene Ontology term metalloendopeptidase activity and Kyoto Encyclopedia of Genes and Genomes pathway ECM–receptor interaction, respectively (Figure 3b). Gene Ontology term ECM component contained significantly downregulated genes, including *COL1A1*, *LAMC2*, and *COL4A6* (Figure 3b). The expression of MMP genes associated with cSCC invasion was investigated further. *MMP1*, *MMP13*, *MMP10*, and *MMP12* were among the significantly downregulated MMP

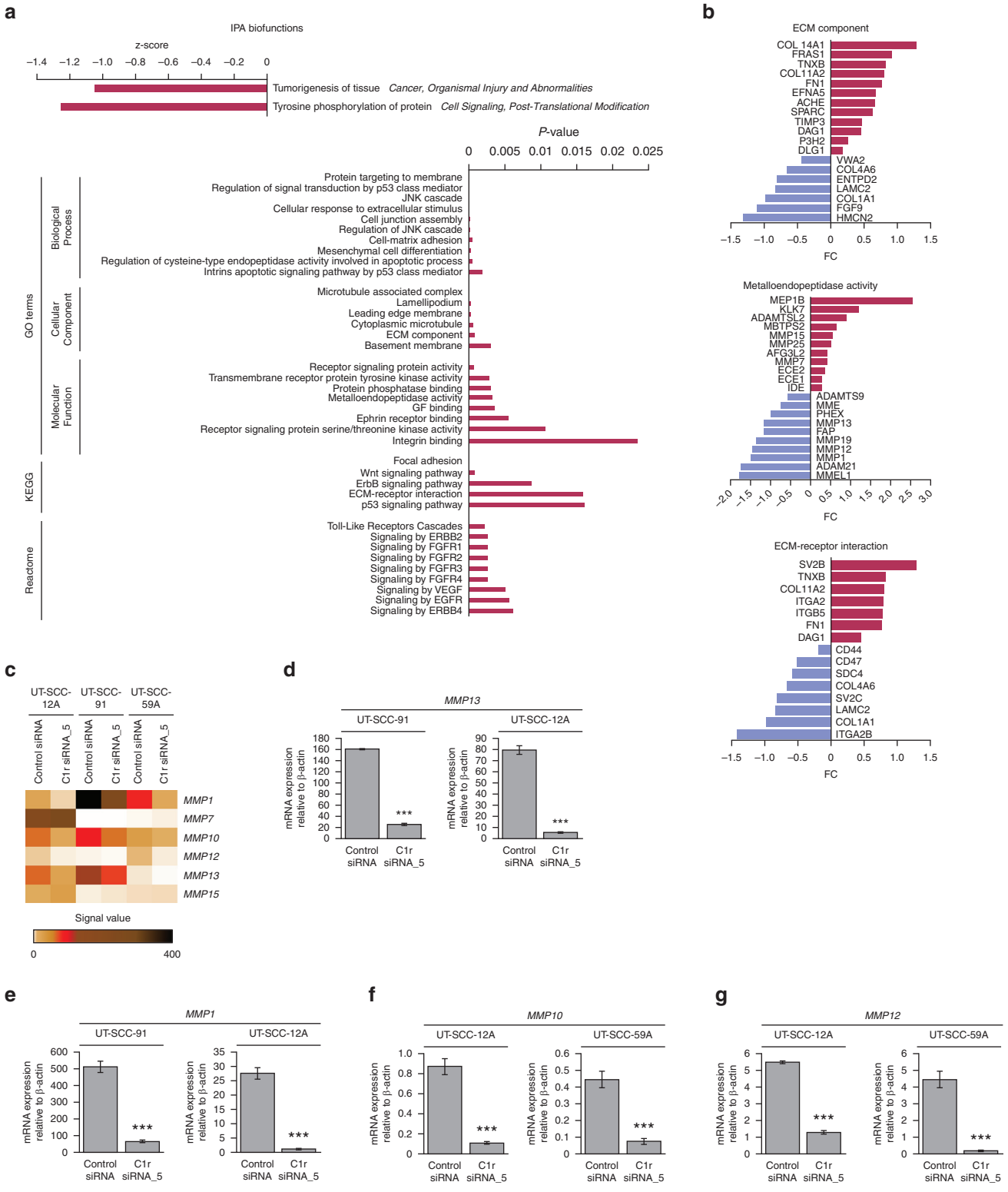

Figure 3. Alteration of gene expression profile in cSCC cells after C1r knockdown. cSCC cell lines (UT-SCC-12A, UT-SCC-91, and UT-SCC-59A) were transfected with C1r siRNA or control siRNA (120 nM), and mRNA-sequencing analysis was performed 72 hours after transfection. (**a**) Summary of IPA biofunctions and GO terms, KEGG pathways, and Reactome related to C1r knockdown ($P < 0.05$, $\log_2$ FC > 1.0). (**b**) Significantly regulated genes belonging to the GO terms ECM component and metalloendopeptidase activity and KEGG pathway ECM-receptor interaction are shown in gene blot. (**c**) Significantly regulated mRNAs for MMPs after C1r knockdown are shown. (**d**) *MMP13*, (**e**) *MMP1*, (**f**) *MMP10*, and (**g**) *MMP12* mRNA levels were determined by QRT-PCR (n = 3). ***$P < 0.001$, Student's *t*-test. cSCC, cutaneous squamous cell carcinoma; ECM, extracellular matrix; FC, fold change; GO, Gene Ontology; IPA, Ingenuity Pathway Analysis; JNK, c-Jun N-terminal kinase; KEGG, Kyoto Encyclopedia of Genes and Genomes; MMP, matrix metalloproteinase; siRNA, short interfering RNA

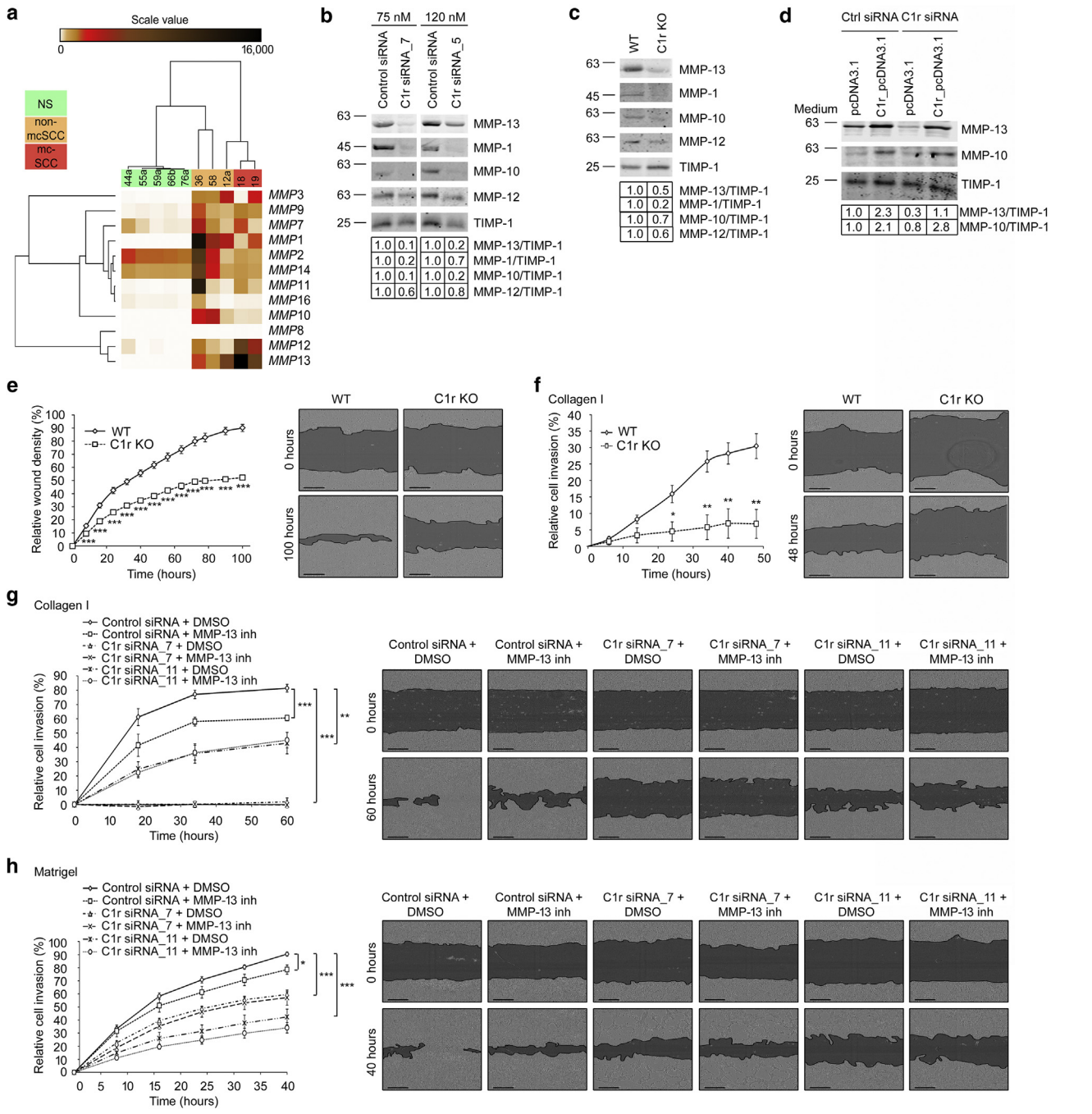

Figure 4. C1r upregulates the production of MMPs and promotes the invasion of cSCC cells. (**a**) Expression of MMP mRNAs in cSCC and normal skin in vivo. RNA samples from human NS (n = 5), nonmetastatic (non-mcSCC, n = 3) cSCC, and metastatic (mcSCC, n = 2) cSCC were analyzed with Nanostring nCounter Fibrosis panel. The data were visualized by hierarchical clustering using Pearson correlation. Relative levels of gene expression are depicted according to the color scale shown. Normalized expression values are shown. (**b**) cSCC cells (UT-SCC-7) were transfected with control or C1r siRNAs, and 72 hours after, transfection levels of MMP-13, MMP-1, MMP-10, and MMP-12 in conditioned media were determined by western blotting. TIMP-1 was used as the loading control. (**c**) MMP-13, MMP-1, MMP-10, and MMP-12 levels were determined in conditioned media of C1r-KO and -WT cSCC cells (UT-SCC-7) by western blotting. TIMP-1 was used as the loading control. (**d**) cSCC cells (UT-SCC-7) were transfected with C1r siRNAs or control siRNA. After 48 hours, cell-conditioned media from C1r-overexpressing (C1r_pcDNA3.1) or vector control (pcDNA3.1) cells was added, and incubation was continued for 24 hours. The levels of MMP-13 and MMP-10 in conditioned media were determined by western blotting. TIMP-1 was used as the loading control. (**e**) To study the migration of C1r-KO and WT cSCC cells (UT-SCC-7), monolayer culture was scratched using 96-well WoundMaker (n = 8). Representative images of the cell migration assay are shown. (**f**) To study the invasion of C1r-KO and WT cSCC cells (UT-SCC-7), monolayer culture was scratched with 96-well WoundMaker, and collagen I solution was added in wells (n = 5–8). Cell invasion was imaged using the IncuCyte ZOOM. Representative images are shown. (**g, h**) cSCC cells were transfected with control or C1r siRNAs, and 48 hours after the transfection, the cell monolayer was scratched using 96-well WoundMaker and **(g)** collagen I (UT-SCC-59A) or (**h**) Matrigel (UT-SCC-91) solution was added in wells (n = 5–7). MMP-13 inh (10 μM) was added to the gel and medium, as indicated. Cell invasion was imaged using the IncuCyte ZOOM or S3 real-time cell imaging system. Representative images are shown. Bar = 300 μm. $*P < 0.05$, $**P < 0.01$, $***P < 0.001$, Student's *t*-test. cSCC, cutaneous squamous cell carcinoma; inh, inhibitor; KO, knockout; mcSCC, metastatic cSCC; MMP, matrix metalloproteinase; NS, normal skin; WT, wild type.

genes after C1r knockdown (Figure 3c). Downregulation of *MMP13*, *MMP1*, *MMP10*, and *MMP12* expression after C1r knockdown was confirmed by QRT-PCR (Figure 3d–g and Supplementary Figure S4a–d).

Expression of MMPs in cSCC in vivo

The expression of MMP genes in vivo in RNA samples of cSCC tumors and normal skin was determined utilizing Nanostring nCounter Fibrosis Panel (Figure 4a). The expression of mRNAs for MMPs, except for *MMP2* and *MMP14*, was higher in cSCCs than in normal skin, and metastatic cSCC samples clustered together (Figure 4a). The mRNA levels of *MMP1*, *MMP10*, *MMP12*, and *MMP13* were upregulated in cSCC compared with those in normal skin (Figure 4a).

C1r upregulates the production of MMPs and promotes the invasion of cSCC cells

The conditioned culture media of C1r-knockdown (Figure 4b) and C1r-KO (Figure 4c) cSCC cells were investigated to determine the production of MMPs. Decreased protein levels of MMP-13, MMP-1, MMP-10, and MMP-12 were detected in the medium of C1r-knockdown (Figure 4b) and C1r-KO (Figure 4c) cSCC cells. The efficiency of C1r siRNAs was analyzed at the protein level in cSCC cells (Supplementary Figure S5).

C1r-overexpressing cSCC cells were generated to rescue C1r expression in C1r siRNA–silenced cells. C1r and C1s expression in the culture medium of C1r-overexpressing (C1r_pcDNA3.1) or vector control (pcDNA3.1) cSCC cells was determined (Supplementary Figure S6). Addition of conditioned medium from C1r-overexpressing cSCC cells to cultures of cells in which *C1r* was silenced resulted in a marked increase in the production of MMP-13 and MMP-10 (Figure 4d). C1r-KO cells showed significantly decreased migration (Figure 4e) and invasion through collagen type I (Figure 4f) compared with WT cSCC cells. C1r knockdown also resulted in significant inhibition of invasion of cSCC cells through collagen type I (Figure 4g and Supplementary Figures S7 and S8a) and Matrigel (Figure 4h and Supplementary Figure S8b). Specific MMP-13 inhibitor inhibited the invasion of control siRNA–transfected cells through collagen I (Figure 4g and Supplementary Figure S8a) and Matrigel (Figure 4h and Supplementary Figure S8b) but had no effect on cell invasion after C1r knockdown.

KO of C1r downregulates the production of MMP-13 by cSCC tumor cells in vivo

C1r-KO and -WT xenografts were stained for histology by H&E and for MMP-13 by immunohistochemistry. Histological analysis of the xenograft tumors revealed different growth and invasion pattern in C1r-KO tumors from those of WT tumors. In WT tumors, cSCC cells were scattered to several smaller islets in 67% of tumors, whereas in C1r-KO xenografts, tumor cells were grouped in larger tumor patches in 83% of tumors (Figure 5a). Positive MMP-13 staining was noted in tumor cells in the invasive edge of xenografts (Figure 5a). The percentage of tumor cells with strong staining for MMP-13 was reduced in C1r-KO tumor margin compared with that in WT tumors (Figure 5a). The area with strong MMP-13–positive staining was quantitated and compared with total tumor area and scored as weak (+), moderate (++), or strong (+++) (Figure 5a and b and Supplementary Figure S9). Of the WT tumors, 33% were scored as strong (+++), 33% were scored as moderate (++), and 33% were scored as weak (+) (Figure 5b). In contrast, of C1r-KO tumors, 17% of cases were classified as strong (+++), 33% were classified as moderate (++), and 50% were classified as weak (+) (Figure 5b).

KO of C1r reduces collagen degradation in cSCC tumors in vivo

To elucidate the effect of downregulation of MMP-13 expression, we determined the amount of total and degraded collagen in xenografts. The total amount of collagen in C1r-KO and WT xenografts was analyzed with van Gieson (VG) staining. An increased amount of short, straight, coarse, and thick collagen bundles was detected in tumor margin between the tumor cells, especially in C1r-KO xenografts (Figure 6a). Xenografts were scored positive (+) if the bundles were detected in more than half of the margin of tumors or negative (−) if the bundles were detected in less than half of the margin of tumors (Figure 6a and b). In 83% of C1r-KO tumors, the short straight, coarse, and thick collagen bundles surrounding cSCC tumor cells indicating an increased amount of collagen were detected in more than half of the tumor edge (Figure 6a and b). In contrast, in WT tumors only in 17% of xenografts, these short straight, coarse, and thick collagen bundles were detected in more than half of the tumor edge (Figure 6a and b).

To further analyze the function of collagenolytic proteinases, such as MMP-13, xenografts were stained with collagen hybridizing peptide (CHP), which specifically binds to degraded, unfolded triple-helical collagen. Association of VG and CHP staining in WT and C1r-KO tumors was analyzed in adjacent sections (Figure 6c). Costaining of VG and CHP was not as strong in C1r-KO tumor group as in WT tumors (Figure 6c). The association was scored positive (+) if the connection was detected in every point and negative (−) if the connection was not detected in every point. In 83% of tumors in WT tumors, the CHP staining in tumor edge was associated with VG staining, indicating degradation of triple-helical collagen molecules (Figure 6c and d). In contrast, in 67% of C1r-KO tumors, there were more areas where CHP staining was not detected, although VG staining was positive, indicating a reduced amount of degraded collagen (Figure 6c and d). Adjacent tissue slide of C1r-KO xenograft tumor was used for negative control staining to exclude nonspecific binding of CHP (Supplementary Figure S10).

DISCUSSION

The complement system is an important part of innate immunity. It can be activated through three pathways, that is, classical, lectin, and alternative pathway, which all lead to the activation of C3 and lytic pathway and eventually to lysis of target cell (Venkatraman Girija et al., 2013). Recently, the role of the complement system in cancer has been emphasized, and the autocrine role of tumor cell–derived complement components in cancer progression has been shown (Afshar-Kharghan, 2017; Cho et al., 2014; Hajishengallis et al., 2017; Kourtzelis and Rafail, 2016; Nissinen et al.,

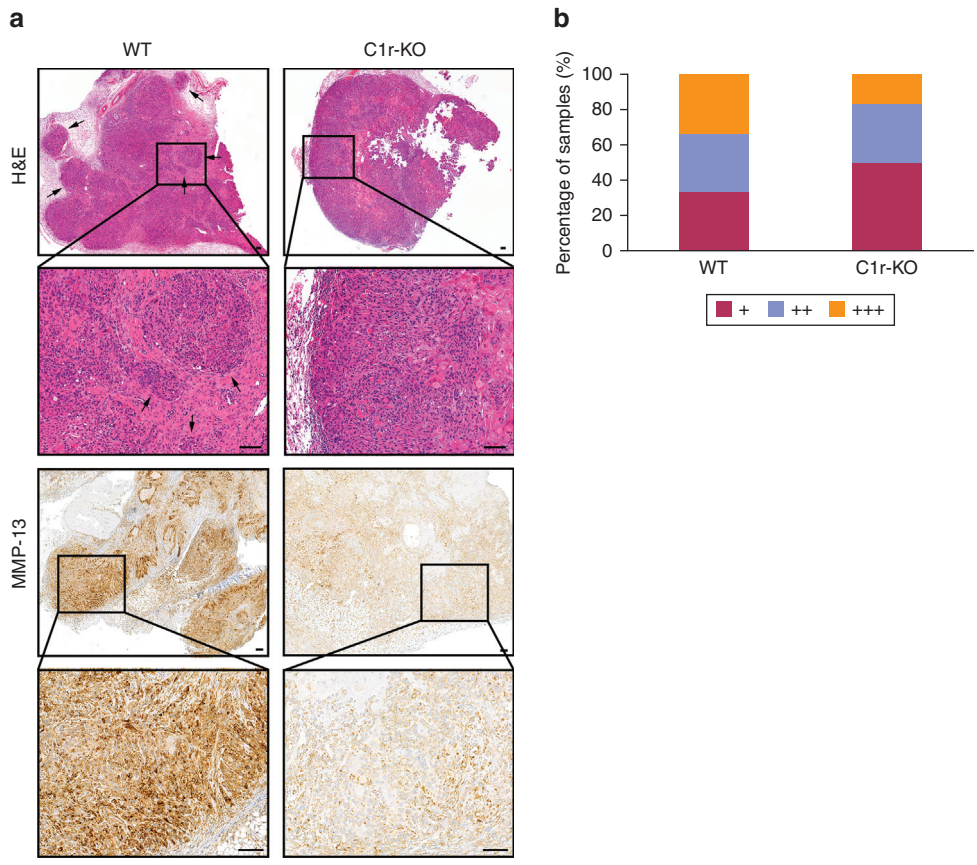

Figure 5. KO of C1r downregulates the production of MMP-13 by cSCC tumor cells in vivo. C1r-KO or -WT UT-SCC-7 cells (7×10^6 cells) were injected subcutaneously into the back of SCID mice (n = 6 for each group). Xenografts were harvested after 17 days and stained with H&E and with immunohistochemistry using an MMP-13 antibody. (**a**) Histological analysis of the xenograft tumors revealed different growth and invasion pattern of C1r-KO tumors compared with that of WT tumors (upper panels). In WT tumors, cSCC cells were scattered to several smaller islets (67% of tumors) (left panels), whereas in C1r-KO xenografts, the tumor cells were grouped in larger tumor patches (83% of tumors) (right panels). Arrows indicate scattered smaller islets in the tumor margin. (**a**) The representative images of strong (+++) MMP-13 staining in WT cSCC tumor cells (lower, left panels). The representative image of weak (+) staining intensity of MMP-13 in C1r-KO tumor cells (right panels). (**b**) The staining intensity of MMP-13 was determined digitally, and the percentage of strongly positive cells was calculated. The area of strong MMP-13–positive staining was measured and compared with total tumor area and scored as weak (+), moderate (++), and strong (+++). Bar = 100 μm. cSCC, cutaneous squamous cell carcinoma; KO, knockout; MMP, matrix metalloproteinase; WT, wild type.

2016; Reis et al., 2018; Roumenina et al., 2019). Our previous studies have shown the autocrine role of cSCC cell–derived complement components C3 and FB and complement inhibitors FH and FI in the proliferation and migration of cSCC cells (Riihilä et al., 2017, 2015, 2014). However, a comparison of the complement expression profiles of different cancers has revealed the unique role of distinct complement components in different cancer types (Roumenina et al., 2019). A number of pharmacological inhibitors against specific complement components are currently in clinical trials and may offer therapeutic approaches to cancer (Riihilä et al., 2019).

We have previously shown that the expression of C1r and C1s is upregulated in tumor cells in cSCC in culture and in vivo (Riihilä et al., 2020). We also showed that cSCC cells do not express C1q subunits, indicating that the autocrine effect of C1r and C1s on cSCC cells is not dependent on the presence of C1q (Riihilä et al., 2020). Furthermore, we have shown that C1s is cleaved and activated in vitro in the absence of C1q (Riihilä et al., 2020). However, several types of cells, for example, macrophages, fibroblasts, and endothelial cells, in the tumor microenvironment of cSCC in vivo can produce C1q subunits (Bossi et al., 2014; Bulla et al., 2016; Petry et al., 2001). It is therefore possible that C1q derived from stromal cells is present in the peritumoral area of cSCC, allowing assembly of $C1qr_2s_2$ complex. It has been shown that locally produced C1q in cancer stroma may be a tumor progression–stimulating factor independently of complement activation (Bulla et al., 2016). We have noted that mRNAs for the *C4* and *C2* components are not expressed by cSCC cells (Riihilä et al., 2014, 2015). Together, these results indicate that components of $C1qr_2s_2$ complex, C1q, C1r, and C1s, may play a specific role in cSCC progression without complement activation.

In this study, we have specifically investigated the mechanistic role of C1r in the progression of cSCC and generated C1r-negative cSCC cells using CRISPR/Cas9. The results show that KO of C1r in cSCC cells results in a significant reduction in viability, proliferation, and invasion of cSCC cells in vitro. In addition, the growth of xenograft tumors established with C1r-negative cSCC cells is significantly suppressed and is associated with reduced vascularization and an increased number of apoptotic tumor cells. Our results also show that reduction in total Akt and ERK1/2 levels results in decreased levels of phosphorylated Akt and phosphorylated ERK1/2 in C1r-KO cells, in accordance with previous studies showing that the components of the ERK1/2 cascade can undergo ubiquitination, which leads to the degradation of the

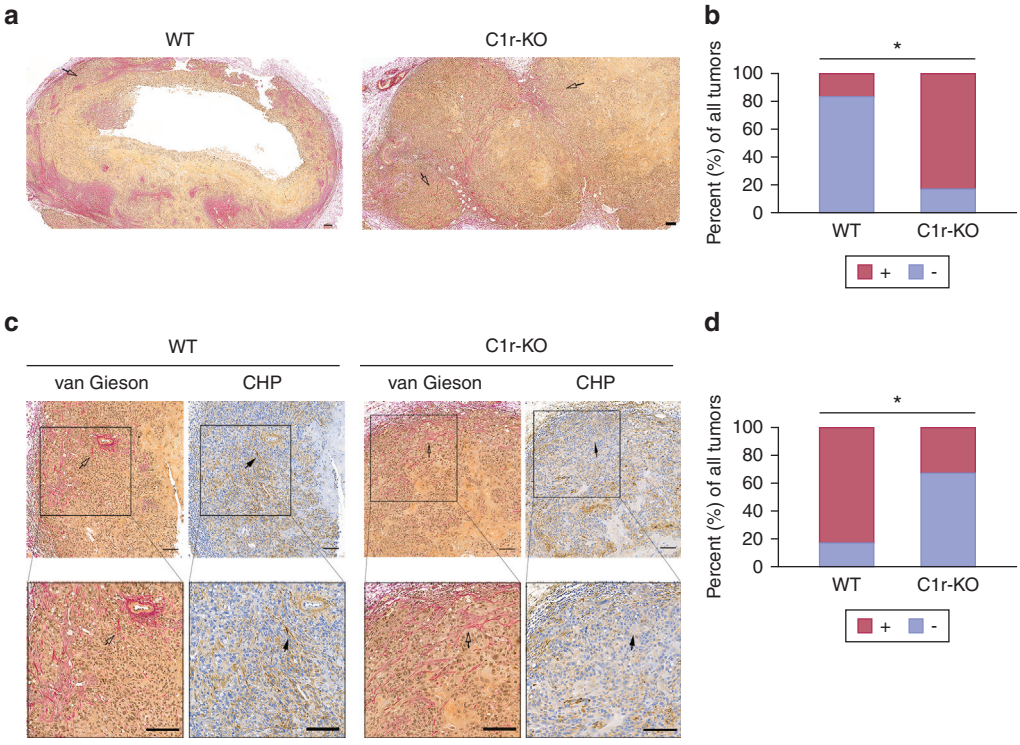

Figure 6. KO of C1r reduces collagen degradation in cSCC in vivo. C1r-KO or -WT UT-SCC-7 cells (7×10^6 cells) were injected subcutaneously into the back of SCID mice (n = 6 for each group) and harvested after 17 days. The total amount of collagen in C1r-KO and WT xenograft tumors was detected with van Gieson staining, and degraded collagen was detected by staining with CHP. (**a**) van Gieson staining in WT and C1r-KO tumors. Short, straight, coarse, and thick collagen bundles were detected in tumor edge rim (white arrows). (**b**) The van Gieson staining was scored positive (+) if short, straight, coarse, and thick collagen bundles were detected in more than a half of the margin of the tumor and negative (−) if short, straight, coarse, and thick collagen bundles were detected in less than a half of the margin of the tumor. (**c**) WT and C1r-KO tumors were stained with CHP. The association of van Gieson (white arrows) and CHP staining (black arrows) was analyzed in adjacent sections of WT and C1r-KO tumors. In WT tumors, the CHP staining in the tumor edge rim was associated with van Gieson staining, as a marker of degraded collagen (left panels). In C1r-KO tumors, there were more areas where CHP staining was not detected, although van Gieson staining was positive, indicating a reduced amount of degraded collagen (right panels). (**d**) The costaining of van Gieson and CHP as a marker of degraded collagen was scored positive (+) if both stainings were detected in every point where short, straight, coarse, and thick collagen bundles were detected and negative (−) if there were points, where a connection was not detected in the tumor margin. Bar = 100 μm. *$P < 0.05$ by χ^2 test (n = 6 for each group). CHP, collagen hybridizing peptide; cSCC, cutaneous squamous cell carcinoma; KO, knockout; WT, wild type.

substrate proteins and also regulates their activity and/or localization (Laine and Ronai, 2005; Lu et al., 2002; Nguyen et al., 2013). Together, these results provide evidence for the important role of C1r in cSCC tumor growth in vivo.

To investigate the molecular mechanism of the effect of C1r in more detail, mRNA sequencing was performed for cSCC cells after C1r knockdown. Knockdown of C1r significantly regulated the genes belonging to Gene Ontology terms related to invasion of cSCC cells, including genes coding for invasion-associated MMPs: *MMP1*, *MMP13*, *MMP10,* and *MMP12*, which are all located in *MMP* gene cluster in locus 11q22.3 (Ujfaludi et al., 2018). Interestingly, the expression of *MMP1*, *MMP13*, *MMP12*, and *MMP10* in cSCC cells is coordinately regulated by signal transducer and activator of transcription 3 (Piipponen et al., 2020). It is conceivable that coordinate upregulation of production of these MMPs by cSCC cells generates a potent proteolytic network in the tumor microenvironment and, this way, promotes invasion of cSCC (Riihilä et al., 2021). It is also possible that these MMPs contribute to alterations in the structure of basement membrane in actinic keratosis and cSCC in situ and, this way, promote their progression to invasive cSCC (Karppinen et al., 2016).

C1r KO inhibited cSCC cell invasion through collagen type I matrix and downregulated production of MMP-1, MMP-13, MMP-10, and MMP-12. Previous studies have shown that MMP-13 (collagenase-3) promotes cSCC progression. MMP-13 cleaves fibrillar collagens and several other ECM and

basement membrane components (Nissinen and Kähäri, 2014; Knäuper et al., 1996a, 1996b). MMP-13 is not expressed in epidermal keratinocytes in normal skin, in normally healing wounds, or in actinic keratosis and cSCC in situ, but the expression is detected in tumor cells and stromal fibroblasts in cSCCs (Airola et al., 1997; Impola et al., 2005; Johansson et al., 1997; Kivisaari et al., 2008; Vaalamo et al., 1997). MMP-13 promotes the growth and invasion of cSCC in vivo, and its expression in cSCC cells is inhibited by p53 (Ala-aho et al., 2004, 2002). In addition, MMP-13 promotes the survival of cSCC cells and fibroblasts (Ala-aho et al., 2004; Toriseva et al., 2007). Our results showed that the expression of MMP-13 by tumor cells in the invasive edges of tumors was decreased in C1r-KO xenografts. In addition, the amount of degraded unfolded triple-helical collagen was decreased in C1r-KO xenograft tumors. In C1r-KO xenografts, tumor cells were grouped in larger nests, whereas in WT tumors, tumor cells were in smaller islets and scattered more widely, indicating that C1r has a role in the shaping of cSCC tumor growth and in invasion pattern in vivo. These results show that loss of C1r in cSCC tumor cells suppresses their MMP-13 production and invasion in vivo.

Our results raise the question of whether the effects of C1r KO are mediated by direct C1r activities or by preventing C1s activation or both. In the extracellular complement system, C1r and C1s are strictly dependent on one another. They are in complex, and activation of C1r is a prerequisite for activation of C1s (Venkatraman Girija et al., 2013). Because the activation of C1r is dependent on conformational change, it is conceivable that it could become activated also intracellularly. Subsequently, C1r could activate C1s, and either of the two or both could have an effect on the expression of MMP-13 or the other MMPs. Thus, because of the similar effects of C1r and C1s knockdowns, it seems possible that at least part of the effects of C1r KO is due to the inability to cleave and activate C1s (Riihilä et al., 2020).

An interesting association between C1 activation and dermal connective tissue has been recognized recently, with the identification of C1r and C1s missense or in-frame insertion/deletion sequence alterations in periodontal Ehlers–Danlos syndrome, a specific autosomally dominantly inherited subtype of Ehlers–Danlos syndrome characterized by severe periodontal inflammation in response to mild plaque accumulation, pretibial hyperpigmentation, acrogeria, skin fragility, and abnormal scarring (Kapferer-Seebacher et al., 2016; Rahman et al., 2003). Examination of the skin of patients with periodontal Ehlers–Danlos syndrome has revealed decreased collagen content, abnormal variation in collagen fibril diameter, and abnormally shaped fibrils, suggesting collagen misassembly and degradation of collagen (Rahman et al., 2003; Reinstein et al., 2013). Interestingly, the C1r and C1s sequence alterations found in patients with periodontal Ehlers–Danlos syndrome are gain-of-function alterations, which result in activation of C1 (Gröbner et al., 2019; Kapferer-Seebacher et al., 2016). These observations provide evidence for the role of C1r in regulating the turnover of dermal collagen.

In summary, the results of this study show that KO of C1r in cSCC cells results in significantly decreased proliferation, migration, and invasion through collagen type I and suppresses the growth of human cSCC xenografts in vivo. In addition, C1r KO decreases the expression of invasion proteinases MMP-1, MMP-13, MMP-10, and MMP-12. These results provide evidence for the role of C1r in regulating the invasion of cSCC cells by increasing the production of invasion-associated MMPs and suggest C1r as a therapeutic target in the treatment of locally advanced and metastatic cSCC.

MATERIALS AND METHODS

Detailed information on Materials and Methods is described in Supplementary Materials and Methods online.

Ethical issues

Collection of cSCC tissues was approved by the Ethics Committee of the Hospital District of Southwest Finland. The research was carried out according to the Declaration of Helsinki. All studied patients gave written informed consent before surgery, and the study was carried out with the authorization of Turku University Hospital (Turku, Finland). All experiments with mice were carried out with the permission of the State Provincial Office of Southern Finland, according to institutional guidelines.

Cell cultures

Human cSCC cell lines were initiated from surgically removed cSCCs (Farshchian et al., 2017). These cell lines were authenticated by STR DNA profiling (Farshchian et al., 2017). Cell cultures were performed, as previously described (Riihilä et al., 2017).

mRNA expression profiling

RNA was isolated using miRNAeasy Mini kit (Qiagen, Chatsworth, CA) from *C1r* and control siRNA (120 nM)-transfected cSCC cell lines (UT-SCC-12A, UT-SCC-91, and UT-SCC-59A). The sequencing library was prepared using Illumina TruSeq Stranded mRNA Sample Preparation Kit, and sequencing was performed using Illumina HiSeq3000 (Illumina, San Diego, CA) at the Finnish Functional Genomics Centre, Turku. The reads were aligned against the human reference genome (hg38), and TMM normalization was used for data normalization (R/Bioconductor package edgeR). For statistical analysis, Limma package was used. RNA-sequencing data (accession number GSE174626) have been deposited in the public database (Gene Expression Omnibus, National Center for Biotechnology Information; http://www.ncbi.nlm.nih.gov/geo/).

Data availability statement

Datasets related to this article can be found at https://www.ncbi.nlm.nih.gov/geo/query/acc.cgi?acc=TBA

ORCIDs

Kristina Viiklepp: http://orcid.org/0000-0002-5895-681X
Liisa Nissinen: http://orcid.org/0000-0002-6743-6736
Marjaana Ojalill: http://orcid.org/0000-0003-3181-6742
Pilvi Riihilä: http://orcid.org/0000-0002-2934-0645
Markku Kallajoki: http://orcid.org/0000-0002-0686-6329
Seppo Meri: http://orcid.org/0000-0001-9142-501X
Jyrki Heino: http://orcid.org/0000-0003-2978-805X
Veli-Matti Kähäri: http://orcid.org/0000-0003-2421-9368

CONFLICT OF INTEREST

The authors state no conflict of interest.

ACKNOWLEDGMENTS

We thank Johanna Markola and Sinikka Collanus for expert technical assistance; Reidar Grénman for cutaneous squamous cell carcinoma cell lines; the Histology Core of the Institute of Biomedicine, University of Turku; and the Bioinformatics Unit and Cell Imaging Core of the Turku Bioscience supported by the University of Turku, Åbo Akademi University, and Biocenter Finland.

This study was funded by Finnish Cancer Research Foundation, Jane and Aatos Erkko Foundation, Sigrid Jusélius Foundation, and Turku University Hospital (projects 13336 and 11027) and by personal funding to PR by Cancer Society of Southwest Finland and to KV from Finnish Cultural Foundation, Ida Montin Foundation, Maud Kuistila Memorial Foundation, Cancer Foundation of Finland, Finnish Dermatological Society, and Turku University Foundation. KV is a doctoral candidate in the Doctoral Programme in Clinical Research at the University of Turku.

AUTHOR CONTRIBUTIONS

Conceptualization: KV, LN, VMK; Funding Acquisition: VMK; Investigation: KV, LN, PR, MK; Methodology; KV, LN, MO, PR; Supervision: LN, PR, VMK; Visualization: KV, LN, PR; Writing - Original Draft Preparation: KV, LN, MO, PR, VMK; Writing - Review and editing; LN, PR, SM, JH, VMK

SUPPLEMENTARY MATERIAL

Supplementary material is linked to the online version of the paper at www.jidonline.org, and at https://doi.org/10.1016/j.jid.2021.10.008.

REFERENCES

Abu-Humaidan AHA, Ananthoju N, Mohanty T, Sonesson A, Alberius P, Schmidtchen A, et al. The epidermal growth factor receptor is a regulator of epidermal complement component expression and complement activation. J Immunol 2014;192:3355–64.

Afshar-Kharghan V. The role of the complement system in cancer. J Clin Invest 2017;127:780–9.

Airola K, Johansson N, Kariniemi AL, Kähäri VM, Saarialho-Kere UK. Human collagenase-3 is expressed in malignant squamous epithelium of the skin. J Invest Dermatol 1997;109:225–31.

Ala-aho R, Ahonen M, George SJ, Heikkilä J, Grénman R, Kallajoki M, et al. Targeted inhibition of human collagenase-3 (MMP-13) expression inhibits squamous cell carcinoma growth in vivo. Oncogene 2004;23:5111–23.

Ala-aho R, Grénman R, Seth P, Kähäri VM. Adenoviral delivery of p53 gene suppresses expression of collagenase-3 (MMP-13) in squamous carcinoma cells. Oncogene 2002;21:1187–95.

Bohlson SS, Garred P, Kemper C, Tenner AJ. Complement nomenclature-deconvoluted. Front Immunol 2019;10:1308.

Bossi F, Tripodo C, Rizzi L, Bulla R, Agostinis C, Guarnotta C, et al. C1q as a unique player in angiogenesis with therapeutic implication in wound healing. Proc Natl Acad Sci USA 2014;111:4209–14.

Bulla R, Tripodo C, Rami D, Ling GS, Agostinis C, Guarnotta C, et al. C1q acts in the tumour microenvironment as a cancer-promoting factor independently of complement activation. Nat Commun 2016;7:10346.

Cho MS, Vasquez HG, Rupaimoole R, Pradeep S, Wu S, Zand B, et al. Autocrine effects of tumor-derived complement. Cell Rep 2014;6:1085–95.

Farshchian M, Nissinen L, Grénman R, Kähäri VM. Dasatinib promotes apoptosis of cutaneous squamous carcinoma cells by regulating activation of ERK1/2. Exp Dermatol 2017;26:89–92.

Gröbner R, Kapferer-Seebacher I, Amberger A, Redolfi R, Dalonneau F, Björck E, et al. *C1R* mutations trigger constitutive complement 1 activation in periodontal Ehlers-Danlos syndrome [published correction appears in Front Immunol 2019;10:2837]. Front Immunol 2019;10:2537.

Hajishengallis G, Reis ES, Mastellos DC, Ricklin D, Lambris JD. Novel mechanisms and functions of complement. Nat Immunol 2017;18:1288–98.

Impola U, Jeskanen L, Ravanti L, Syrjänen S, Baldursson B, Kähäri VM, et al. Expression of matrix metalloproteinase (MMP)-7 and MMP-13 and loss of MMP-19 and p16 are associated with malignant progression in chronic wounds. Br J Dermatol 2005;152:720–6.

Johansson N, Airola K, Grénman R, Kariniemi AL, Saarialho-Kere U, Kähäri VM. Expression of collagenase-3 (matrix metalloproteinase-13) in squamous cell carcinomas of the head and neck. Am J Pathol 1997;151:499–508.

Kapferer-Seebacher I, Pepin M, Werner R, Aitman TJ, Nordgren A, Stoiber H, et al. Periodontal Ehlers-Danlos syndrome is caused by mutations in C1r and C1s, which encode subcomponents C1r and C1s of complement. Am J Hum Genet 2016;99:1005–14.

Karia PS, Han J, Schmults CD. Cutaneous squamous cell carcinoma: estimated incidence of disease, nodal metastasis, and deaths from disease in the United States, 2012. J Am Acad Dermatol 2013;68:957–66.

Karppinen SM, Honkanen HK, Heljasvaara R, Riihilä P, Autio-Harmainen H, Sormunen R, et al. Collagens XV and XVIII show different expression and localisation in cutaneous squamous cell carcinoma: type XV appears in tumor stroma, while XVIII becomes upregulated in tumor cells and lost from microvessels. Exp Dermatol 2016;25:348–54.

Kivisaari AK, Kallajoki M, Mirtti T, McGrath JA, Bauer JW, Weber F, et al. Transformation-specific matrix metalloproteinases (MMP)-7 and MMP-13 are expressed by tumour cells in epidermolysis bullosa-associated squamous cell carcinomas. Br J Dermatol 2008;158:778–85.

Knäuper V, López-Otín C, Smith B, Knight G, Murphy G. Biochemical characterization of human collagenase-3. J Biol Chem 1996a;271:1544–50.

Knäuper V, Will H, López-Otín C, Smith B, Atkinson SJ, Stanton H, et al. Cellular mechanisms for human procollagenase-3 (MMP-13) activation. Evidence that MT1-MMP (MMP-14) and gelatinase A (MMP-2) are able to generate active enzyme. J Biol Chem 1996b;271:17124–31.

Knuutila JS, Riihilä P, Kurki S, Nissinen L, Kähäri VM. Risk factors and prognosis for metastatic cutaneous squamous cell carcinoma: a cohort study. Acta Derm Venereol 2020;100:adv00266.

Kourtzelis I, Rafail S. The dual role of complement in cancer and its implication in anti-tumor therapy. Ann Transl Med 2016;4:265.

Laine A, Ronai Z. Ubiquitin chains in the ladder of MAPK signaling. Sci STKE 2005;2005:re5.

Lu Z, Xu S, Joazeiro C, Cobb MH, Hunter T. The PHD domain of MEKK1 acts as an E3 ubiquitin ligase and mediates ubiquitination and degradation of ERK1/2. Mol Cell 2002;9:945–56.

Nagarajan P, Asgari MM, Green AC, Guhan SM, Arron ST, Proby CM, et al. Keratinocyte carcinomas: current concepts and future research priorities. Clin Cancer Res 2019;25:2379–91.

Navratil JS, Watkins SC, Wisnieski JJ, Ahearn JM. The globular heads of C1q specifically recognize surface blebs of apoptotic vascular endothelial cells. J Immunol 2001;166:3231–9.

Nehal KS, Bichakjian CK. Update on keratinocyte carcinomas. N Engl J Med 2018;379:363–74.

Nguyen LK, Kolch W, Kholodenko BN. When ubiquitination meets phosphorylation: a systems biology perspective of EGFR/MAPK signalling. Cell Commun Signal 2013;11:52.

Nissinen L, Farshchian M, Riihilä P, Kähäri VM. New perspectives on role of tumor microenvironment in progression of cutaneous squamous cell carcinoma. Cell Tissue Res 2016;365:691–702.

Nissinen L, Kähäri VM. Matrix metalloproteinases in inflammation. Biochim Biophys Acta 2014;1840:2571–80.

Petry F, Botto M, Holtappels R, Walport MJ, Loos M. Reconstitution of the complement function in C1q-deficient (C1qa−/−) mice with wild-type bone marrow cells. J Immunol 2001;167:4033–7.

Piipponen M, Nissinen L, Riihilä P, Farshchian M, Kallajoki M, Peltonen J, et al. p53-regulated long noncoding RNA PRECSIT promotes progression of cutaneous squamous cell carcinoma via STAT3 signaling [published correction appears in Am J Pathol 2020;190:916]. Am J Pathol 2020;190:503–17.

Que SKT, Zwald FO, Schmults CD. Cutaneous squamous cell carcinoma: incidence, risk factors, diagnosis, and staging. J Am Acad Dermatol 2018;78:237–47.

Rahman N, Dunstan M, Teare MD, Hanks S, Douglas J, Coleman K, et al. Ehlers-Danlos syndrome with severe early-onset periodontal disease (EDS-VIII) is a distinct, heterogeneous disorder with one predisposition gene at chromosome 12p13. Am J Hum Genet 2003;73:198–204.

Ratushny V, Gober MD, Hick R, Ridky TW, Seykora JT. From keratinocyte to cancer: the pathogenesis and modeling of cutaneous squamous cell carcinoma. J Clin Invest 2012;122:464–72.

Reinstein E, DeLozier CD, Simon Z, Bannykh S, Rimoin DL, Curry CJ. Ehlers–Danlos syndrome type VIII is clinically heterogeneous disorder associated primarily with periodontal disease, and variable connective tissue features. Eur J Hum Genet 2013;21:233–6.

Reis ES, Mastellos DC, Ricklin D, Mantovani A, Lambris JD. Complement in cancer: untangling an intricate relationship. Nat Rev Immunol 2018;18:5–18.

Ricklin D, Hajishengallis G, Yang K, Lambris JD. Complement: a key system for immune surveillance and homeostasis. Nat Immunol 2010;11:785–97.

Riihilä P, Nissinen L, Farshchian M, Kallajoki M, Kivisaari A, Meri S, et al. Complement component C3 and complement factor B promote growth of cutaneous squamous cell carcinoma. Am J Pathol 2017;187:1186–97.

Riihilä P, Nissinen L, Farshchian M, Kivisaari A, Ala-Aho R, Kallajoki M, et al. Complement factor I promotes progression of cutaneous squamous cell carcinoma. J Invest Dermatol 2015;135:579–88.

Riihilä P, Nissinen L, Kähäri VM. Matrix metalloproteinases in keratinocyte carcinomas. Exp Dermatol 2021;30:50–61.

Riihilä P, Nissinen L, Knuutila J, Rahmati Nezhad P, Viiklepp K, Kähäri VM. Complement system in cutaneous squamous cell carcinoma. Int J Mol Sci 2019;20:3550.

Riihilä P, Viiklepp K, Nissinen L, Farshchian M, Kallajoki M, Kivisaari A, et al. Tumour-cell-derived complement components C1r and C1s promote growth of cutaneous squamous cell carcinoma. Br J Dermatol 2020;182:658–70.

Riihilä PM, Nissinen LM, Ala-aho R, Kallajoki M, Grénman R, Meri S, et al. Complement factor H: a biomarker for progression of cutaneous squamous cell carcinoma. J Invest Dermatol 2014;134:498–506.

Roumenina LT, Daugan MV, Petitprez F, Sautés-Fridman C, Fridman WH. Context-dependent roles of complement in cancer. Nat Rev Cancer 2019;19:698–715.

Rutkowski MJ, Sughrue ME, Kane AJ, Ahn BJ, Fang S, Parsa AT. The complement cascade as a mediator of tissue growth and regeneration. Inflamm Res 2010;59:897–905.

Toriseva MJ, Ala-aho R, Karvinen J, Baker AH, Marjomäki VS, Heino J, et al. Collagenase-3 (MMP-13) enhances remodeling of three-dimensional collagen and promotes survival of human skin fibroblasts. J Invest Dermatol 2007;127:49–59.

Ujfaludi Z, Tuzesi A, Majoros H, Rothler B, Pankotai T, Boros IM. Coordinated activation of a cluster of MMP genes in response to UVB radiation. Sci Rep 2018;8:2660.

Vaalamo M, Mattila L, Johansson N, Kariniemi AL, Karjalainen-Lindsberg ML, Kähäri VM, et al. Distinct populations of stromal cells express collagenase-3 (MMP-13) and collagenase-1 (MMP-1) in chronic ulcers but not in normally healing wounds. J Invest Dermatol 1997;109:96–101.

Venkatraman Girija U, Gingras AR, Marshall JE, Panchal R, Sheikh MA, Harper JA, et al. Structural basis of the C1q/C1s interaction and its central role in assembly of the C1 complex of complement activation [published correction appears in Proc Natl Acad Sci USA 2016;113:E6722–3]. Proc Natl Acad Sci USA 2013;110:13916–20.

SUPPLEMENTARY MATERIALS AND METHODS

Knockout of C1r

To generate C1r-negative cell lines, genome editing method was applied by transfecting UT-SCC-7 cells with an all-in-one CRISPR/Cas9 vector (Sigma-Aldrich, St Louis, MO, HS0000245574 guide RNA sequence: GCTTCACCCTG-TATCCCGTGGG; HS0000245577 guide RNA sequence: ACTTCTCCAACGAGGAGAATGG). Transfected cells were selected on the basis of the expression of GFP, allowed to grow, and checked for C1r and C1s production in a cell culture medium. Four *C1r*-knockout (KO) cutaneous squamous cell carcinoma (cSCC) single-cell clones (C1r CRISPR 74_1, 74_2, 74_3, and 77_3) were pooled to generate C1r-KO cell line.

Tissue RNA

Normal human skin samples (n = 5) were obtained from the upper arm of healthy volunteers or during mammoplasty operation in Turku University Hospital (Turku, Finland). Human primary nonmetastatic (n = 3) and metastatic (n = 2) cSCC samples were collected from surgically removed tumors in Turku University Hospital (Riihilä et al., 2020). Total RNA was isolated from the tissue samples as previously described (Riihilä et al., 2020).

Nanostring expression profiling

RNA (100 ng) was hybridized overnight at 65 °C with the Human Fibrosis Panel (NanoString Technologies, Seattle, WA). Purification and binding of the hybridized probes to the cartridge were performed on the nCounter Prep Station, followed by scanning the cartridge on the nCounter Digital Analyzer (NanoString Technologies). The data analysis was prepared using nSolver 4.0 (NanoString Technologies). The quality of the data was confirmed; normalization was done using the default quality control settings.

QRT-PCR

Total RNA was isolated and analyzed by QRT-PCR, as previously described (Riihilä et al., 2020). The mRNA levels of matrix metalloproteinases (MMPs), *MMP1*, *MMP10*, *MMP12*, *MMP13*, and β-actin were analyzed by QRT-PCR using specific primers as described earlier (Stokes et al., 2010). The samples were analyzed in duplicate, and the range of the threshold cycle values was <5% of the mean in each measurement. The mRNA levels of MMPs were corrected for levels of β-actin mRNA.

Western blotting analysis

Production of C1r and C1s by cSCC cells was determined by western blotting analysis of aliquots of conditioned media under nonreducing conditions using specific polyclonal rabbit anti-C1r (HPA001551; Sigma-Aldrich) and anti-C1s (HPA018852; Sigma-Aldrich) antibodies. Production of MMPs was determined by western blotting analysis of aliquots of conditioned media under reducing conditions using specific antibodies against MMP-1 (41-1E5; Merck Millipore, Temecula, CA), MMP-10 (IVC5; Thermo Fisher Scientific, Waltham, MA), MMP-12 (MAB919; R&D Systems, Minneapolis, MN) and MMP-13 (Ab-3; Merck Millipore). With TIMP-1 antibody (Ab-1; Merck Millipore), equal protein loading was confirmed. Cell lysates were analyzed with antibodies specific for phosphorylated protein kinase B (Akt), phosphorylated extracellular signal–regulated kinase (ERK)-1/2, total ERK1/2 (9271S, 9101, and 9102, all from Cell Signaling Technology, Beverly, MA), and total Akt (sc-1618, Santa Cruz Biotechnology, Santa Cruz, CA) by western blotting. Even protein loading was firmed with β-actin antibody (A1978; Sigma-Aldrich).

Knockdown of C1r expression with short interfering RNA

For short interfering RNA (siRNA) knockdown of C1r, cSCC cells were grown to 50% confluency and transfected with siRNAs targeting *C1R* mRNA (target sequences: Hs_C1r_5, 5′-TCGGGAGAGCCCAGGATTCAA-3′ [120 nM]; Hs_C1r_7, 5′-CAGGGTGAAGCTCGTCTTCCA-3′ [75 nM]; and Hs_C1r_11, 5′-CCAGTTGTTGATSSCCACTAA-3′) (75 nM) or with negative control siRNA (all from Qiagen, New Delhi, India) using siLentFect Lipid Reagent (Bio-Rad Laboratories, Hercules, CA) as previously described (Riihilä et al., 2020). The function of C1r siRNAs was verified by western blotting. β-Actin served as a loading control, and quantitation of western blot band intensities was carried out by ImageJ software, version 1.47v (National Institutes of Health, Bethesda, MD; http://imagej.nih.gov/ij) (Schneider et al., 2012).

mRNA expression profiling

RNA was isolated using miRNAeasy Mini kit (Qiagen, Chatsworth, CA) from C1r- and control siRNA (120 nM)-transfected cSCC cell lines (UT-SCC-12A, UT-SCC-91, and UT-SCC-59A). The sequencing library was prepared using Illumina TruSeq Stranded mRNA Sample Preparation Kit, and sequencing was performed using Illumina HiSeq3000 (Illumina, San Diego, CA) at the Finnish Functional Genomics Centre, Turku. The reads were aligned against the human reference genome (hg38), and TMM normalization was used for data normalization (R/Bioconductor package edgeR). For statistical analysis, Limma package was used. RNA-sequencing data (accession number GSE174626) have been deposited in the public database (Gene Expression Omnibus, National Center for Biotechnology Information; http://www.ncbi.nlm.nih.gov/geo/).

Overexpression of C1r

C1R nucleotide sequence was obtained from National Center for Biotechnology Information. The *C1R* cDNA fragment in pEX-A128 was ordered from Eurofins Genomics (Ebersberg, Germany) and cloned into pcDNA3.1 (Invitrogen, Carlsbad, CA) comprising neomycin resistance gene. To validate the integrity of cloned *C1R* segment, the construct was resequenced. Stable transfections of UT-SCC-7 cells with the recombinant C1r expression construct (pcDNA3.1_C1r) or control vector (pcDNA3.1) were performed using Lipofectamine 3000 reagent (Invitrogen, Carlsbad, CA) (Piipponen et al., 2018). Cells were grown in the presence of 0.5 mg/ml of geneticin (Gibco, Waltham, MA). In a rescue experiment, cSCC cells were transfected with C1r siRNAs or control siRNA. After 48 hours, the conditioned media of C1r-overexpressing (C1r_pcDNA3.1) or vector control (pcDNA3.1) cells were added, and incubation continued for 24 hours.

Cell number and viability assays

UT-SCC-7 C1r-KO and wild-type (WT) cells (5.0×10^3 cells per well) were inoculated into 96-well plates. The IncuCyte

ZOOM real-time cell imaging system (Essen BioScience, Ann Arbor, MI) was used to study the growth of cSCC cells. Images were taken every 2 hours by IncuCyte ZOOM, and the relative confluence was analyzed by the instrument. Experiments were carried out with eight parallel wells at every time point. For cell viability assays, cSCC cells (1.0×10^4 cells per well) were seeded on 96-well plates. The number of viable cells was determined at 0, 24, 48, and 72 hours with Cell Counting Kit-8 (Dojindo Laboratories, Kumamoto, Japan). Experiments were carried out with eight parallel wells at every time point.

Cell migration assays

UT-SCC-7 C1r-KO and -WT cells (3.5×10^4 cells per well) were plated on ImageLock 96-well plate (Essen BioScience, Ann Arbor, MI) and incubated in a complete growth medium for 24 hours to reach confluency. Cell division was inhibited by treatment with 1 mM hydroxyurea (Sigma-Aldrich) treatment in DMEM with 10% fetal calf serum for 6 hours. After that, the cell monolayer was scratched with IncuCyte ZOOM (Essen BioScience) wound scratcher, and incubation of the cells was continued in DMEM with 1% fetal calf serum and 0.5 mM hydroxyurea. Images were taken every 2 hours by IncuCyte ZOOM, and the relative wound density was analyzed by the instrument. Experiments were carried out with eight parallel wells at every time point.

Cell invasion assay

cSCC cells (5×10^4 cells per well) were plated on a collagen type I (5 μg/cm2, PureCol; Advanced BioMatrix, San Diego, CA) or Matrigel (100 μg/ml) (Corning, Corning, NY)-coated ImageLock 96-well plate (Essen BioScience) 24 hours after transfection with C1r siRNAs or negative control siRNA. C1r-KO and -WT cells and siRNA-transfected cells were allowed to adhere overnight. The cell monolayer was scratched, and Matrigel (4 mg/ml) (UT-SCC-7 and UT-SCC-59A) or collagen type I (UT-SCC-7 and UT-SCC-91) solution was added by mixing type I collagen (PureCol) with ×5DMEM and 0.2 mol/l 4-(2-hydroxyethyl)-1-piperazineethanesulfonic acid buffer (pH 7.4) at a ratio of 7:2:1, respectively. Sodium hydroxide (1 M) was added to obtain a final pH of 7.4. Cell culture medium with 0.5% fetal calf serum was added after allowing the collagen type I solution (2.2 mg/ml) to polymerize for 2 hours at 37 °C. MMP-13 inhibitor (444283, Merck, Darmstadt, Germany) was added to the gel and medium in 10 μM concentration. Images were taken every 2 hours by IncuCyte ZOOM or S3 real-time cell imaging system, and the relative cell invasion was quantitated using the IncuCyte ZOOM or S3 software (Essen BioScience). Experiments were carried out with 6–7 parallel wells at every time point.

Human cSCC xenografts

Human cSCC xenografts were established, as described previously (Riihilä et al., 2017). UT-SCC-7 C1r-KO or WT cells (5×10^6) were injected subcutaneously in the back of severe combined immunodeficiency (SCID/SCID) female mice ($n = 6$ in both groups) (CB17/Icr-*Prkdc*^{scid}/IcrIcoCrl) (Charles River LaboratoriesWilmington, MA). The size of tumors was measured twice a week, and tumor volume was calculated with the formula $V = (\text{length} \times \text{width}^2) / 2$ (Euhus et al., 1986). Tumors were harvested after 17 days for histological analysis and immunohistochemistry, as previously described (Riihilä et al., 2017). Proliferating cells were detected with monoclonal human Ki-67 antibody (MIB-1; DAKO, Glostrup, Denmark), and Mayer's hematoxylin was used as counterstain. The relative number of Ki-67–positive cells was determined by counting 1,400–4,900 cells from all sections at ×20 objective using ImageJ software (Schneider et al., 2012). Vascularization of the xenograft tumors was assessed by immunohistochemistry with anti-CD34 antibody (Santa Cruz Biotechnology). Blood vessel density was evaluated in each sample by counting the number of CD34-positive blood vessels in three defined microscopic fields at ×10 objective. Apoptosis of the xenograft tumor cells was determined by immunohistochemistry with active caspase-3 antibody (Cell Signaling Technology, Danvers, MA). The relative number of active caspase-3–positive cells was determined by counting 4,800–8,750 cells from all sections at ×20 objective using ImageJ software (Schneider et al., 2012).

MMP-13 stainings were performed with mouse monoclonal MMP-13 antibody (MAB13424; Merck Millipore). To evaluate the MMP-13 staining intensity in xenograft tumor tissue sections, QuPath bioimage analysis software, version 0.2.3, was used (Bankhead et al., 2017). Strong MMP-13 staining was distinguished digitally by creating threshold 0.4, which detects only strong staining on the basis of DAB staining intensities. The areas of strong staining intensity were measured and compared with whole-xenograft tumor areas to calculate the percentage of strong positive staining of xenograft tumor. Tumors were scored as weak (+), moderate (++), and strong (+++) on the basis of the percentage of strong MMP-13 staining. The staining was classified as weak (+) if the strong MMP-13 staining accounted for <4% of xenograft tumor area, moderate (++) if the strong staining area was 4–9%, and strong if the area was >9%.

To visualize collagen paraffin-embedded, formalin-fixed WT and C1r-KO xenograft tumor sections were stained with van Gieson and collagen hybridizing peptide-biotin conjugate (B-CHP, BIO300, 3Helix, Salt Lake City, Utah) according to manufacturer's instructions (Hwang et al., 2017). The specificity of collagen hybridization of CHP was tested using negative control. For negative control staining, trimeric CHP solution without the preheating step was added to the sample to not dissociate CHP trimers from monomers by heating.

All tissue samples were stained at the same time, and immunohistochemical detection was performed using Labvision Autostainer to standardize the staining quality and intensity. The stainings were performed in Core Facilities of the Institute of Biomedicine, University of Turku, as previously described (Riihilä et al., 2020). The slides of xenograft samples were digitally scanned using a Panoramic 1000 Slide Scanner (3DHistech, Budapest, Hungary).

SUPPLEMENTARY REFERENCES

Bankhead P, Loughrey MB, Fernández JA, Dombrowski Y, McArt DG, Dunne PD, et al. QuPath: open source software for digital pathology image analysis. Sci Rep 2017;7:16878.

Euhus DM, Hudd C, LaRegina MC, Johnson FE. Tumor measurement in the nude mouse. J Surg Oncol 1986;31:229–34.

Hwang J, Huang Y, Burwell TJ, Peterson NC, Connor J, Weiss SJ, et al. In situ imaging of tissue remodeling with collagen hybridizing peptides. ACS Nano 2017;11:9825–35.

Piipponen M, Heino J, Kähäri VM, Nissinen L. Long non-coding RNA PICSAR decreases adhesion and promotes migration of squamous carcinoma cells by downregulating α2β1 and α5β1 integrin expression. Biol Open 2018;7: bio037044.

Riihilä P, Nissinen L, Farshchian M, Kallajoki M, Kivisaari A, Meri S, et al. Complement component C3 and complement factor B promote growth of cutaneous squamous cell carcinoma. Am J Pathol 2017;187: 1186–97.

Riihilä P, Viiklepp K, Nissinen L, Farshchian M, Kallajoki M, Kivisaari A, et al. Tumour-cell-derived complement components C1r and C1s promote growth of cutaneous squamous cell carcinoma. Br J Dermatol 2020;182:658–70.

Schneider CA, Rasband WS, Eliceiri KW. NIH Image to ImageJ: 25 years of image analysis. Nat Methods 2012;9:671–5.

Stokes A, Joutsa J, Ala-aho R, Pitchers M, Pennington CJ, Martin C, et al. Expression profiles and clinical correlations of degradome components in the tumor microenvironment of head and neck squamous cell carcinoma. Clin Cancer Res 2010;16:2022–35.

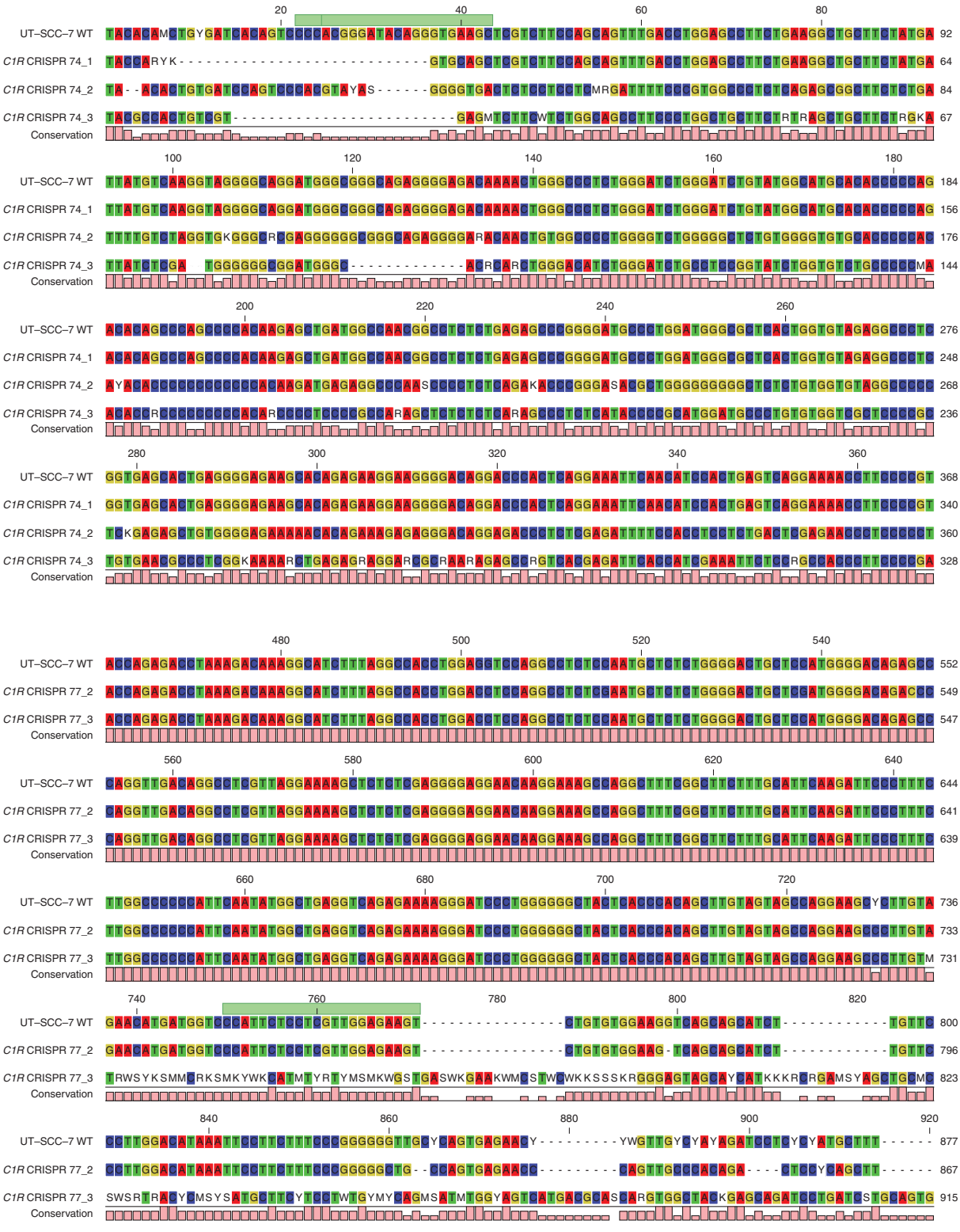

Supplementary Figure S1. DNA Sanger sequencing of control and mutated cSCC cells (UT-SCC-7) after C1R knockout. Top row of chromatograms represents a part of WT *C1R*-gene. Bottom rows on chromatograms represent mutated *C1R* gene sequences from one-cell clones. Guide RNA and PAM sequence in CRISPR/Cas9 vector are shown in green. Comparison confirms apparent changes of DNA sequences around the cutting site in single-cell clones generated with CRISPR/Cas9. cSCC, cutaneous squamous cell carcinoma; PAM, protospacer adjacent motif; WT, wild-type.

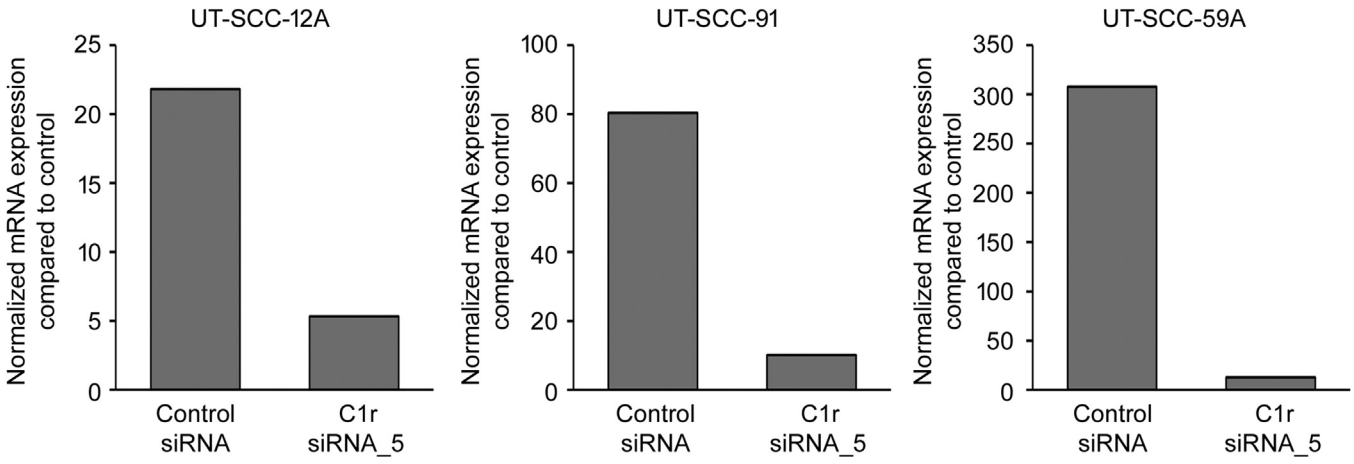

Supplementary Figure S2. Expression of C1r in cSCC cells after C1r knockdown. cSCC cell lines (UT-SCC-12A, UT-SCC-91, and UT-SCC-59A) were transfected with control or C1r siRNA_5 (120 nM). At 72 hours after transfection, mRNA-seq analysis was performed. Normalized *C1R* mRNA expression was determined from cSCC cells with mRNA-seq after C1r siRNA knockdown. cSCC, cutaneous squamous cell carcinoma; mRNA-seq, mRNA sequencing; siRNA, short interfering RNA.

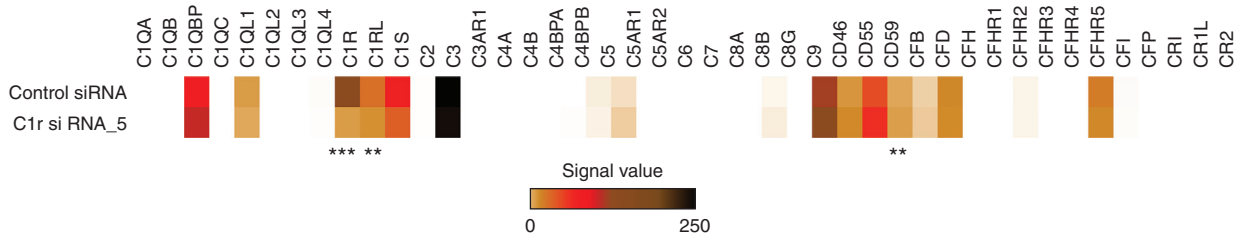

Supplementary Figure S3. Alteration of the expression of complement-related genes in cSCC cells after C1r knockdown. cSCC cells (UT-SCC-12A, UT-SCC-91, and UT-SCC-59A) were transfected with control siRNA or C1r siRNA_5 (120 nM), and mRNA sequencing was performed 72 hours after transfection. Heatmap shows the expression of complement-related genes after C1r knockdown. (**$P < 0.01$ and ***$P < 0.001$, R package Limma). cSCC, cutaneous squamous cell carcinoma; siRNA, short interfering RNA.

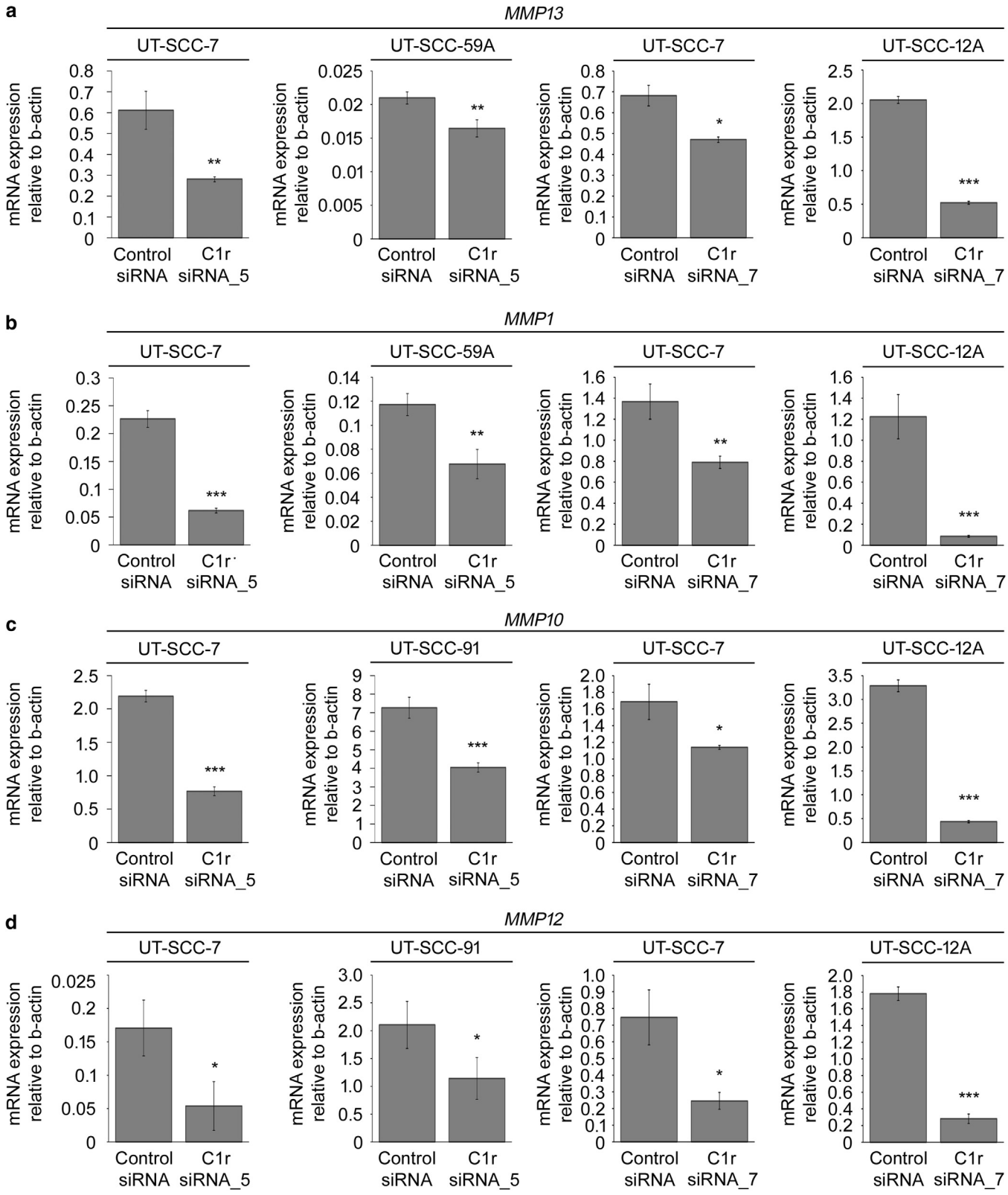

Supplementary Figure S4. C1r knockdown decreases the expression of *MMP13, MMP1, MMP10,* and *MMP12* in cSCC cells. cSCC cell lines (UT-SCC-7, UT-SCC-12A, UT-SCC-59A, and UT-SCC-91) were transfected with C1r siRNA_5 (120 nM), C1r siRNA_7 (75 nM), or control siRNA, and QRT-PCR was performed 72 hours after transfection. MMP mRNA **(a)** *MMP13*, **(b)** *MMP1*, **(c)** *MMP10*, and **(d)** *MMP12* levels were determined (n = 3, $*P < 0.05$, $**P < 0.01$, $***P < 0.001$, Student's *t*-test). cSCC, cutaneous squamous cell carcinoma; MMP, matrix metalloproteinase; siRNA, short interfering RNA.

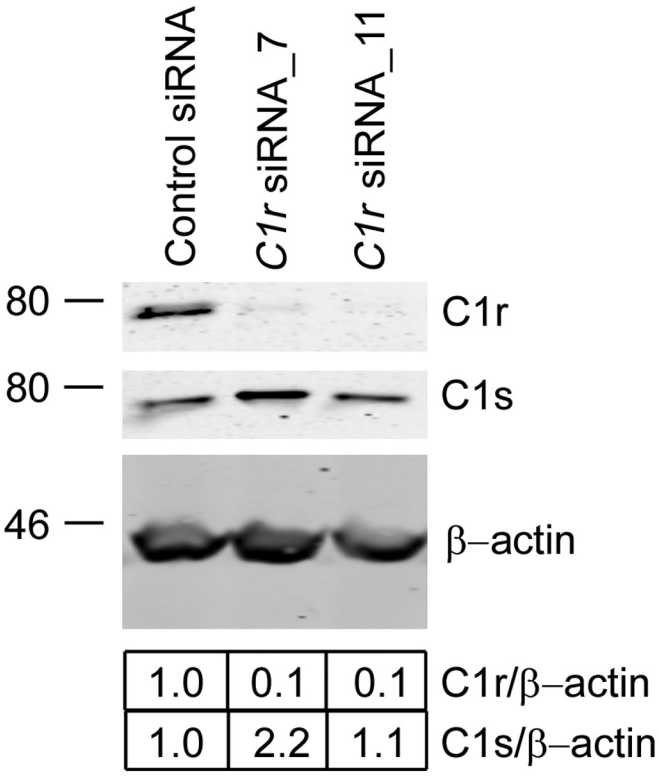

Supplementary Figure S5. The efficiency of C1r siRNAs was analyzed at the protein level in cSCC cells. cSCC cells (UT-SCC-7) were transfected with C1r siRNA (C1r siRNA_7 or C1r siRNA_11) or control siRNA (75 nM). Conditioned media were analyzed for C1r and C1s levels 8 days after transfections by western blotting. β-Actin was used as a sample control. Densitometric quantitation of C1r and C1s levels corrected for β-actin is shown below the panels. cSCC, cutaneous squamous cell carcinoma; siRNA, short interfering RNA.

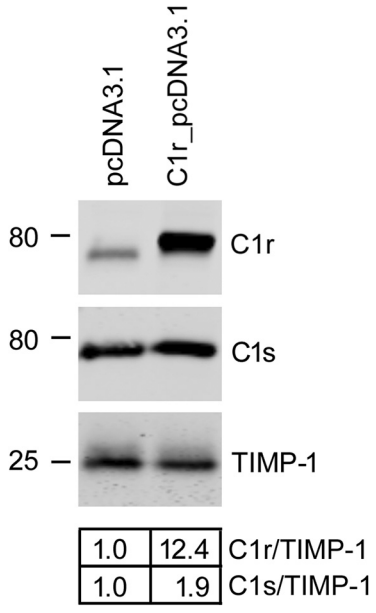

Supplementary Figure S6. Expression of C1r and C1s in *C1r*-overexpressing cSCC cells. The levels of C1r and C1s in conditioned culture media collected from C1r-overexpressing (C1r_pcDNA3.1) and vector control (pcDNA3.1) UT-SCC-7 cells were determined by western blotting. TIMP-1 was used as the loading control. Densitometric quantitation of C1r and C1s levels corrected for TIMP-1 are shown below the panels. cSCC, cutaneous squamous cell carcinoma.

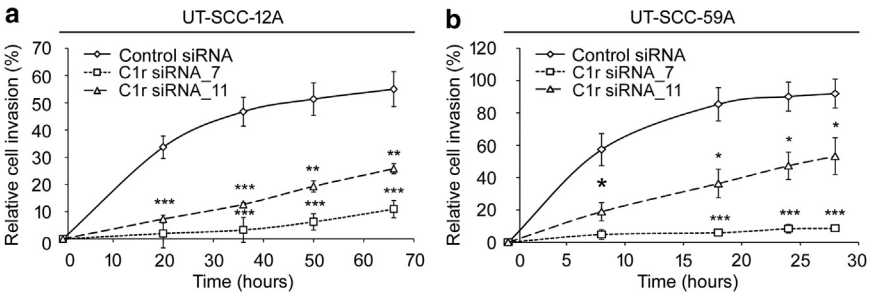

Supplementary Figure S7. Knockdown of C1r inhibits the invasion of cSCC cells by collagen I. cSCC cells (UT-SCC-12A and UT-SCC-59A) were transfected with C1r or control siRNAs (75 nM). At 48 hours after transfection, the cell monolayer was scratched using 96-well WoundMaker, and collagen I solution was added in wells. Cell invasion was imaged using the IncuCyte ZOOM (n = 5–8, $*P < 0.05$, $**P < 0.01$, $***P < 0.001$, Student's *t*-test.). cSCC, cutaneous squamous cell carcinoma; siRNA, short interfering RNA.

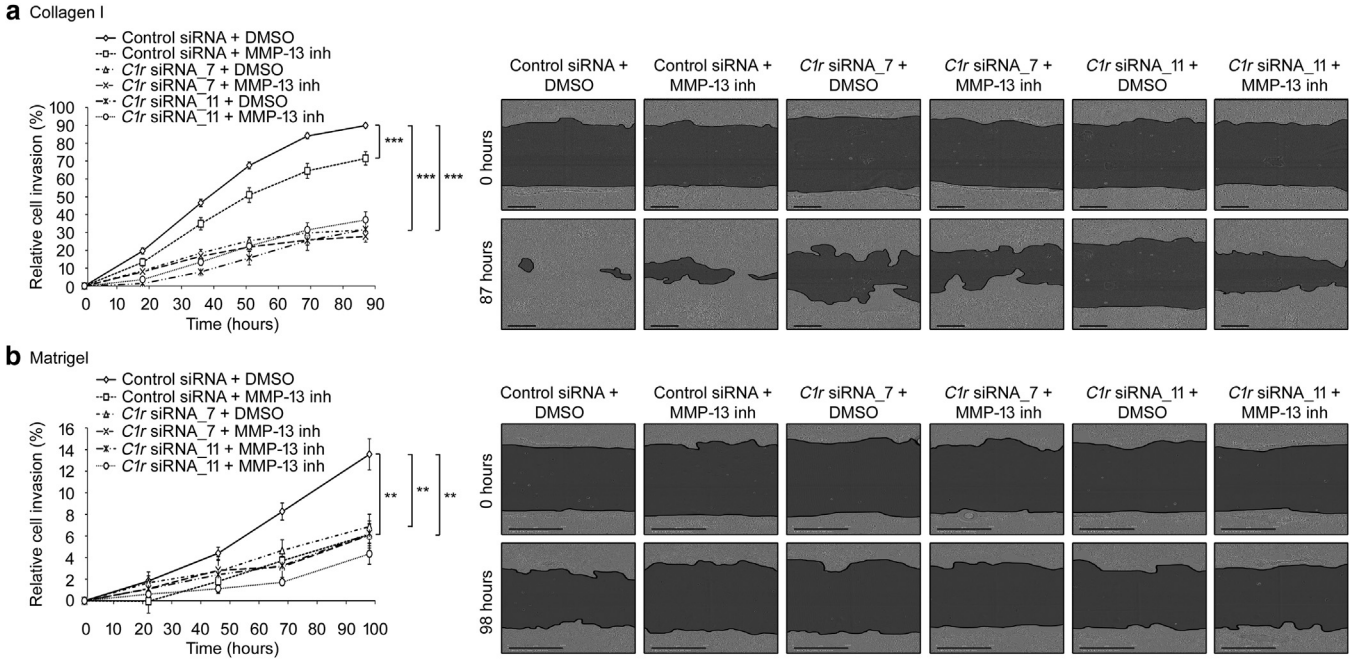

Supplementary Figure S8. C1r promotes the invasion of cSCC cells by increasing their production of MMP-13. cSCC (UT-SCC-7) cells were transfected with control or C1r siRNAs, and 48 hours after transfection, the cell monolayer was scratched using 96-well WoundMaker, and **(a)** collagen I or **(b)** Matrigel solution was added in wells. MMP-13 inh was added to the gel and medium at 10 μM concentration. Cell invasion was imaged using the IncuCyte ZOOM or S3 real-time cell imaging system. Representative images are shown. Bar = 300 μm. n = 5–7; $**P < 0.01$, $***P < 0.001$, Student's *t*-test. cSCC, cutaneous squamous cell carcinoma; inh, inhibitor; MMP, matrix metalloproteinase; SCC, squamous cell carcinoma; siRNA, short interfering RNA.

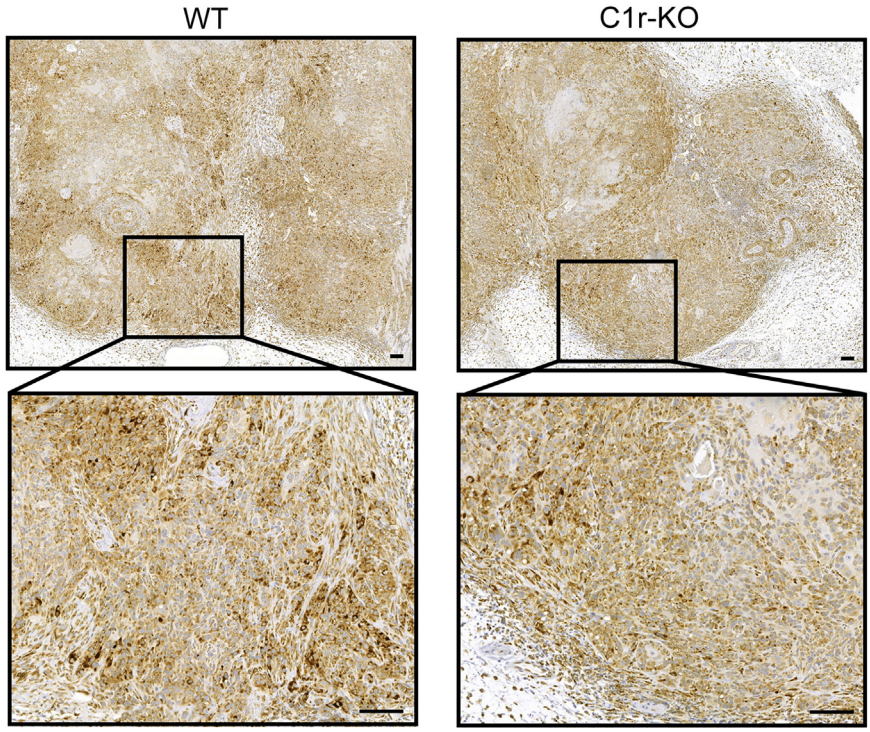

Supplementary Figure S9. Moderate (++) MMP-13 staining intensity in cSCC WT and C1r-KO xenograft tumor cells. C1r-KO or -WT cSCC cells (UT-SCC-7) (7×10^6 cells) were injected subcutaneously into the back of SCID mice, harvested after 17 days, and stained with anti–MMP-13. The areas of strong staining intensity of MMP-13 were quantitated digitally and compared with total tumor areas and scored as weak (+), moderate (++), and strong (+++). Representative images of moderate (++) staining in WT (left panel) and in C1r-KO (right panel) tumors are shown. Bar = 100 μm. cSCC, cutaneous squamous cell carcinoma; inh, inhibitor; KO, knockout; MMP, matrix metalloproteinase; WT, wild type.

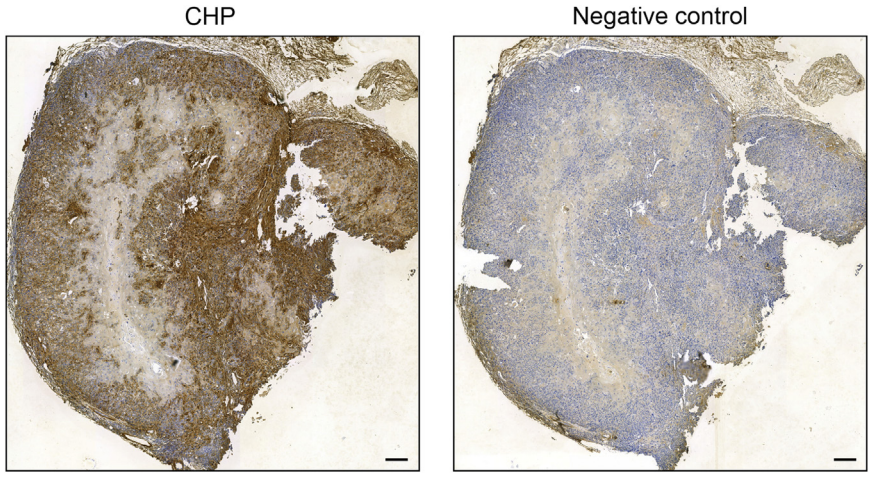

Supplementary Figure S10. Detection of degraded collagen in cSCC xenograft tumor. C1r-KO cSCC cells (UT-SCC-7) (7×10^6 cells) were injected subcutaneously into the back of SCID mice and harvested after 17 days. A xenograft tumor was stained with CHP (left panel). An adjacent tissue slide was used for negative control staining to exclude nonspecific binding of CHP. CHP stain was added to sample slide without the preheating step (right panel). Bar = 200 μm. CHP, collagen hybridizing peptide; cSCC, cutaneous squamous cell carcinoma; KO, knockout.